Design and Testing of a High Frequency Hydraulic Mechanical Jackhammer

By Stephen McGuire

Presented to the Department of Bioresource Engineering of McGill University
In Partial fulfillment of the requirements
for the Degree of Master of Science

McGill University, Macdonald Campus
Montreal, Quebec, Canada

Abstract

Concrete has been used as a building material for thousands of years. The material has continued to evolve in parallel with our growing understanding of internal structural stresses. As one of the primary building materials in urban centres, concrete is routinely poured, repaired, and demolished. Expansive agents, hydraulic splitting, hydraulic demolition and mechanical demolition breakers are common methods of concrete removal, as documented by Abudayyeh, Sawhney et al. in 1998. Mechanical demolition breakers, known as jackhammers, are commonly used within the industry as they provide a versatile platform for the reduction in size of large quantities of material. The first patent for a pneumatic jackhammer was granted to Charles King in 1894. This design depicts a machine with an internal hammer that is pushed back and forth by compressed air. On the downward stroke the hammer contacts a chisel which transfers the impact energy into the concrete, inducing fracture of the material. As early as 1929, Holtzmann began to document the development of degenerative arthritis in workers who used hand held demolition breaker. Despite the machine's noise, and ergonomic issues, the jackhammer has not seen substantial redesign or development over the past century.

In 1969, Benjumea and Sikarskie developed a model of the crushing and chipping process that occurs after the impact of a rigid chisel on a brittle material such as concrete or granite. This model clearly showed a primary crushing and secondary chipping process following the impact of the chisel. Dutta, in 1972, modeled the geometric indentation of the crushing and chipping zones as being dependant on the geometry of the chisel tip and the material being impacted. A more in-depth understanding of the upper and lower limits of the crushing and chipping sequence as well as the effect of repeated impacts was developed by Pang, Goldsmith and Hood in 1989. These models took into consideration the material characteristics, chisel geometry, and force with which the chisel is struck. They made the assumption that the time delay between strikes will have little impact on the indentation geometry.

The research in this thesis, developed and tested a high frequency hydraulic mechanical jackhammer capable of reaching impact frequencies of over 80 Hz, more than doubling the impact frequencies of a single hammer. This machine implemented a design using two hammer mechanisms connected to a single tip. Ultimately the design increased the impact frequency by 2.3 times without modifying the chisel tip geometry or striking force. Testing demonstrated that the design was functional and material indentation did occur. Further testing is required following the methods outlined by Pang and Goldsmith in 1990 to determine if the crack propagation at elevated frequencies is in accordance with the indentation models outlined in the literature.

Resumé

Le béton est utilisé comme matériau de construction depuis des milliers d'années. Ce matériau a évolué parallèlement à notre compréhension croissante des contraintes structurelles internes. En tant que principal matériau de construction dans les centres urbains, le béton est coulé, réparé et démoli de manière routinière. Les agents expansifs, l’éclatement hydraulique, la démolition hydraulique et la démolition mécaniques sont des méthodes courantes d'élimination du béton, comme le documentaient Abudayyeh, Sawhney et al. en 1998. Les marteaux de démolition mécaniques, appelés marteaux-piqueurs, sont couramment utilisés dans l'industrie, car ils fournissent une plate-forme polyvalente pour la réduction de la taille de grandes quantités de matériaux. Le premier brevet pour un marteau-piqueur pneumatique a été accordé à Charles King en 1894. Cette conception représente une machine avec un marteau interne poussé à un mouvement de va-et-vient par de l'air comprimé. Lors de la descente, le marteau entre en contact avec un burin qui transfère l'énergie de l'impact au béton, induisant une rupture du matériau. Dès 1929, Holtzmann commença à documenter le développement de l'arthrose chez les travailleurs qui utilisaient des marteaux-piqueurs portatifs. Malgré le bruit de la machine et les problèmes d’ergonomie, le marteau-piqueur n’a pas connu de nouvelle conception ni de développement substantiel au cours du siècle dernier.

En 1969, Benjumea et Sikarskie élaborèrent un modèle du processus d’écrasement et de burinage qui se produit après l’impact d’un burin rigide sur un matériau fragile tel que le béton ou le granit. Ce modèle montre clairement un processus de broyage primaire et de burinage secondaire après l’impact du burin. En 1972, Dutta a modélisé l’indentation géométrique des zones de broyage et de burinage en fonction de la géométrie de la pointe du burin et du matériau

impacté. Pang, Goldsmith et Hood ont développé en 1989 une compréhension plus approfondie des limites supérieure et inférieure de la séquence de concassage et de burinage ainsi que de l'effet des impacts répétés. Ces modèles prenaient en compte les caractéristiques du matériau, la géométrie du burin et la force avec laquelle le burin frappe. Ils ont fait l’hypothèse que le délai entre les frappes aurait peu d'impact sur la géométrie de l'indentation.

Les travaux de recherche dans cette thèse ont permis de mettre au point et d’essayer un marteau-piqueur mécanique hydraulique de haute fréquence capable d’atteindre des fréquences d’impact supérieures à 80 Hz, soit plus du double des fréquences d’impact d’un marteau. Cette machine a mis en œuvre une conception utilisant deux mécanismes de marteau connectés à une seule pointe. La conception a augmenté la fréquence d’impact de 2,3 fois sans modifier la géométrie de la pointe du burin ni la force de frappe. Les essais ont démontré que la conception était fonctionnelle et qu'une indentation matérielle s'était produite. Des essais supplémentaires sont nécessaires selon les méthodes décrites par Pang et Goldsmith en 1990 pour déterminer si la propagation de la fissure à des fréquences élevées est conforme au modèle d'indentation indiqué dans la littérature.

Contribution of Authors

For this thesis the contribution of authors are such as: (1) Stephen McGuire – designed and built the high-frequency jackhammer, designed and conducted experiments, data collection, and explanation of results; (2) Dr. Mark Lefsrud – supervision during the design, construction, and testing of the high-frequency jackhammer, provided guidance, knowledge and revision of thesis.

Acknowledgements

It is important to take the time to recognize those who have contributed to our success. Most importantly, to recognize the influence they have had on our personal development and therefore the tools that we continue to use throughout our lives. I would like to thank Dr. Lefsrud for his approach to problem solving and his mentality of contributing to society as an engineer. Without his willingness to push boundaries, this project would remain nothing more than an idea. I would like to thank Matthew Pittaro and Acra Concrete Services Inc. Matt has been supportive of the project and understanding of the obstacles faced during testing. I would like to thank the Bioresource Engineering Department at Macdonald College. Their value of theoretical and applied learning has allowed students from many backgrounds to build and test their theories in the real world. A personal thanks must be given to Scott Manktelow for all the help and guidance that he has provided at the Macdonald Campus Engineering Shop. Without Scott, I would not have the ability to fabricate and troubleshoot a machine such as this. Lastly, I would like to thank Michael, Helen, and Jacklyn for their support throughout this process.

Table of Contents

List of Figures

List of Tables

List of Abbreviations

BPM - Beats Per Minute

RPM - Revolutions per Minute

LPM - Litres per Minute

SDS - Slotted Drive System

1 Introduction

1.1 Background

Concrete functions as a primary building material in urban centres around the world. As the global population continues to increase, the use of concrete will remain instrumental to society's industrial development as a whole (MIT, 2019). Concrete is a composite material constituted primarily of cement, sand, gravel, and water (Guo, 2014). Once cured, these components form two material zones; aggregate and cement paste. Depending on the application and environment, different additives may be incorporated to increase the concrete's flowability, strength, lifespan, or even resistance to environmental conditions (Atici and Ersoy, 2008). Concrete degrades over time due to environmental conditions, improper maintenance, excessive wear, and chemical degradation (Dawood et al., 2018). Depending on the extent of the damage, partial or complete removal of the existing material may be required to re-establish structural integrity (El-Salakawy, Polak, and Soudki, 2002).

Demolition and removal of degraded concrete is common around the world (Lerard and Colina, 2019). However, it can cause substantial disturbance in urban areas (Carpenter, 2018). Concrete, which is highly resistant to compressive forces, requires high energy impact to induce crack propagation (Pang and Goldsmith, 1990). The impact energy is not only disturbing at close range but may also resonate within structures. For these reasons, municipal governments have placed restrictions on concrete demolition practices, to limit the disturbance it can cause to neighboring businesses or residential buildings (Gannoruwa, Ruwanpura, 2007).

Many different methods of concrete demolition have been developed for use within the urban landscape. These methods include expansive agents (e.g. calcium oxide), hydraulic splitting, hydro-demolition, as well as hydraulic, pneumatic, or electro-mechanical breakers (Abudayyeh, Sawhney, El-Bibany, and Buchanan, 1998). All these methods utilize a specific technology that is applicable to different demolition requirements and material conditions. The mechanisms of demolition that are applied within these technologies will be reviewed with a focus on the modern demolition breaker.

The first patent for a demolition breaker, or jackhammer, was submitted by Charles B. King on the 30th of January 1894 (King, 1894). His patent used compressed air to move an internal piston back and forth, while striking a chisel on the downward stroke (King, 1894). This machine was the first of its kind and resembles a foundation that modern jackhammers have been built on.

Operators of a jackhammer may be at risk for long term joint deterioration. As early as 1929, Holtzmann began to document the development of degenerative arthritis in workers who used hand held demolition breakers (Fam and Kolin, 1986). The reciprocating action of the internal piston, coupled with the high frequency vibration of the chisel strike, can lead to deteriorating joint structures and even result in internal organ issues (Copeman, 1940; Shields and Chase, 1988).

Despite advances in fabrication techniques and manufacturing, the design of the modern-day demolition hammer remains very similar to its original concept (Pang and Goldsmith, 1990). Furthermore, demolition has proven to be more difficult in modern urban centers (Carpenter, 2018). This research was performed to develop a better understanding of modern systems and how impact frequency may be increased in order to improve demolition efficiency.

1.2 Statement of Research Objectives

The objective of this research is to review modern demolition methods, their physical mechanisms of demolition, and to develop new technology that is less disruptive to both the operator and the surrounding environment.

- Objective 1

  Perform a full literature review of modern demolition technology and asses the mechanisms that are used for the demolition of concrete.

- Objective 2

  Design and build a hydraulic mechanical jackhammer capable of reaching higher impact frequencies than commercially available machines.

- Objective 3

  Operate the machine at impact frequencies of at least 75 Hz and observe its functionality with respect to the demolition of concrete.

1.3 Choice of Methodology

Concrete is a complex, heterogeneous material that can vary considerably depending on the region, curing methods, component mixtures and aggregate quality (Guo, 2014). While considering these variables, it was deemed necessary to build and test an original high frequency hydraulic mechanical jackhammer, rather than develop a mathematical simulation of the effects of high frequency impact on concrete. The design of this machine was structured around obtaining high impact frequencies at the chisel tip of the jackhammer, while only slightly modifying the mechanism that induces impact upon the concrete. A machine capable of producing impact frequencies of over 75 Hz, will be considered "high frequency" for this study. The machine was designed for short testing sequences and many modifications to the machine's drivetrain were necessary to allow the machine to operate for a sufficient period.

Operational data was collected via audio recording and visual observation, following completion of the test sequence. This testing was done to confirm the functionality of the machine, while further testing will be required to properly determine the machine's efficiency. This portion of the research was conducted in order to design and test the functionality of a multi-head mechanism and observe demolition at elevated impact frequencies.

This machine was tested concrete that was mixed to the manufacturer's specifications with a compressive strength of 27.6 MPa. Three rectangular samples of concrete were poured with dimensions of 70 cm in length, by 70 cm in width, by 35 cm in height. The samples were impacted on the largest face with dimensions of 70 cm by 70 cm. This sample size proved to be manageable and provided enough mass so that the sample could absorb the impact energy, resulting only in local fracture. All material used for this experiment belonged to the same mixture and was cured in a nearly identical environment, to the manufacturer's specifications, to ensure that sample variance was minimized.

1.4 Organization of Thesis

The preparation of this thesis has been separated into three major components that will be represented in five chapters. Chapter 1 will review the background information and significance of this research. Chapter 2 will include a review of the literature pertaining to all methods of concrete demolition and their efficiencies. Next, Chapters 3 and 4 will examine the design, fabrication, as well as the testing procedure and results of the prototype hammer itself. Finally, in Chapter 5, the existing technology, prototype performance, and future recommendations for the research will be summarized. This thesis has been organized in a manner to sequentially present the information required to understand the design process, its innovation, as well as the development of new technology that has occurred throughout the realization of this research.

2 Review of Technology

2.1 Review of Concrete and Material Characteristics

Concrete has been documented as a construction material for thousands of years. The oldest known sample of concrete was found in Yugoslavia and dates more than 7500 years (Mallinson and Davies, 1987). In modern society, concrete provides a financially viable option for large scale construction. Reinforced concrete provides a low maintenance, cost effective, highly durable, and versatile building material (Aoyama, 2001).

Concrete is a composite material that is constituted primarily of cement, sand, gravel, and water (Guo, 2014). These components are mixed together, cast, and cured to form the material that is commonly known as concrete. The manufacturing process and component materials' characteristics can have a major effect on the structural rigidity of the final product. Due to its complex variable matrix of composite materials, concrete is heterogeneous (Guo, 2014).

Structurally reinforced concrete implements a framework of steel reinforcement bar, re-bar, around which the concrete is formed and cured (Guo, 2014). This structure provides strength to the concrete material where the internal stress is predominantly tensile. Meanwhile, the concrete itself is highly resistant to compressive loads. Structurally reinforced concrete offers many advantages to non-reinforced concrete and has been used as a construction method for the past century (Aoyama, 2001). The astonishing adoption of reinforced concrete in structural engineering design is due to the mating of both materials providing increased strength.

2.2 Material Strength and Properties

Concrete must be allotted time to cure once it has been cast. It is important that adequate curing conditions are provided over a specific duration, that considers both the temperature and the humidity of the surrounding environment. Despite continuing to cure indefinitely, concrete is deemed to have reached its cured strength after 28 days (Aoyama, 2001). Depending on the mixture, aggregate quality, air temperature and humidity of the curing environment, concrete can demonstrate varying yield strengths. Concrete ranges from 25 MPa to 90 MPa compressive strength, depending upon specific mix ratios and composition (Carino, Guthrie, and Lagergren, 1994). Given its compressive strength of greater than 41 MPa, it is deemed to be high strength concrete, as per the American Concrete Institute (Mendis, 2003). A Poisson's ratio of 0.2 and a modulus of elasticity of 40 GPa for unfractured concrete is recommended for design purposes (Brooks, 2015).

The tensile strength of concrete is much lower than its compressive strength. Thus, the material does not resist compression and tension in a similar manner (Guo,2014). As the tensile stress increases, the tensile Poisson's ratio of the concrete decreases; the opposite is true for compressive stresses in concrete (Guo, 2014). For this reason, concrete members are designed to demonstrate extreme strength under compressive forces but require reinforcement when in tension. Re-bar is therefore used to increase the tensile strength of the material (Pothisiri and Panedpojaman, 2012). Re-bar is generally composed of mild steel and placed within the cast before the concrete has been poured. Ridges in the reinforcement bar are essential to the structural bond between the two materials, as the cohesion between the concrete and steel is limited during the curing process (Pothisiri and Panedpojaman, 2012). Depending on the design of the structure, the size, type and amount of rebar can vary considerably and is modeled during the structural design phase (Cho, Lee, and Bae, 2014).

2.3 Demolition Methods

Concrete demolition has become a vast industry during the 21st century due to the use of concrete as a common building material (Larrard and Colina, 2019). Massive sections of reinforced concrete must be broken down into portions that can be transported on public roads or repurposed on site. Jackhammers are common place within this industry and provide a robust platform for the demolition of material (Abudayyeh, Sawhney, El-Bibany, and Buchanan, 1998). Many methods of demolition of concrete exist. Some of these include; hydraulic demolition (Momber, 2005), expansive demolition agents (Gambatese, 2003), hydraulic rock splitters (Abudayyeh et al., 1998), as well as hydraulic, electromechanical, and pneumatic demolition breakers or jackhammers (Suprenant, 1991). Each of these demolition methods provide benefits in specific work environments. Given the versatility and robust characteristics of the modern demolition breaker and jackhammer, it is the most commonly used tool when performing the demolition of a concrete structure (Abudayyeh et al., 1998).

2.3.1 Hydro Demolition

Hydro demolition methods consist of using a high-pressure jet of water to wear away at the material. Development on this demolition process first began in the late 1980's and has since become a common method of partial material removal (Abudayyeh et al., 1998). At pressures of over 100 MPa, a water jet is capable of intruding into the material to remove weakened portions of the structure (Momber, 2005). Hydro-demolition can erode material that has been weakened from environmental factors while leaving structurally sound material intact. The surface that remains is rough enough to provide bonding between old and new material, without damaging the rebar in the demolition process (Figure 2.3.1). These systems require upwards of 260 litres per minute to operate (Momber, 2005). Due to environmental requirements on construction sites, this volume must be treated or collected post demolition.

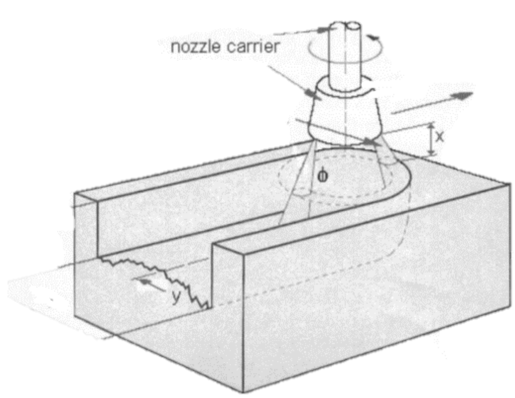

Figure 2.3.1 Hydro-demolition process showing a
high-pressure jet deteriorating the concrete surface.
(Momber, 2005)

Due to the nature of hydraulic demolition, its application is primarily for the removal of surface material or portions of a structure that are undergoing refurbishment. Low noise levels, minimal labour and a relatively high demolition rate establishes this method as an interesting solution to common demolition drawbacks. This method does not exert high energy impact into the concrete and is therefore much less likely to result in excessive crack propagation within the material (Abudayyeh et al., 1998).

2.3.2 Mechanical and Chemical Expansive Demolition

When the use of traditional demolition is limited, it is often replaced with agents such as expansive demolition or soundless chemical demolition. Expansive demolition agents serve as a viable option, given their reductions in noise and vibrational disturbance, as well as their enhanced precision of debris removal. This method consists of drilling holes in the concrete and filling them with a mixture of chemical agents. Typically, this includes an agent that consist of lime, calcium oxide, that is mixed with an additional agent such as aluminum oxide, in order to moderate the rate of hydration (Gambatese, 2003). When the mixture is subsequently subjected to water, the expansion process begins. During expansion, increased stress is placed on the walls of the drilled holes, eventually inducing fracture (Harada, Idemitsu, and Watanabe, 1985)(Figure 2.3.2). Soundless chemical demolition agents can be used to provide localized, non-intrusive

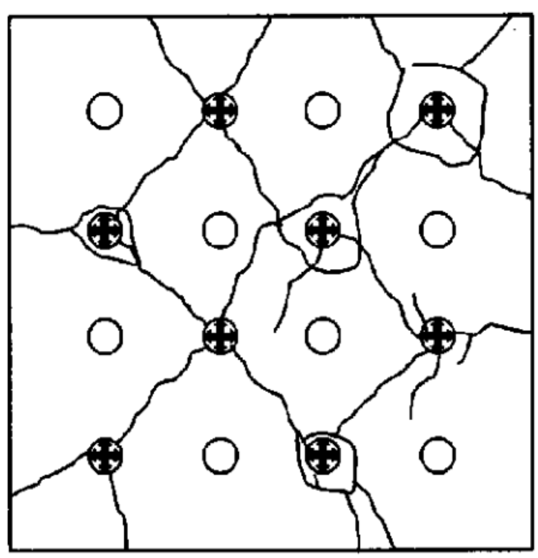

Figure 2.3.2 Hole placement and crack formation during the use of expansive agents or hydraulic splitters (Gambatese, 2003).

removal of material from a larger structure (Gambatese, 2003). Issues surrounding the use of expansive demolition are primarily concerning the extended process that is required for demolition. The material must be drilled, injected with the chemical agent, hydrated, and let sit until the expansion has induced cracking (Harada, Idemitsu, Watanabe, and Takayama, 1989). Due to increased complexity and the reduced rate of demolition, expansive agents are rarely used if traditional methods can be implemented (Abudayyeh et al., 1998).

Hydraulic splitters implement a similar breaking method to expansive agents. However, they utilize hydraulic mechanisms to apply pressure to the inside wall of the holes drilled in the material. These mechanisms resemble a two-piece wedge with a small hydraulic ram in the centre. The hydraulic ram pushes in a forward direction, separating the two-piece wedge, while placing immense pressure on the wall of the hole. Forces exerted on the outside wall can exceed 3650 kN (Abudayyeh et al., 1998). Similar time constraints are required for site preparation, yet the crack propagation can be completed faster relative to expansive agents. Minimal noise levels in combination with localised material fracture is possible. Restrictions are seen when limited crack propagation occurs due to rebar present within the material (Abudayyeh et al., 1998). In comparison to traditional methods, the hydraulic splitters cannot provide similar results in a distinct timeline (Abudayyeh et al., 1998).

2.3.3 Demolition Breakers and Jackhammers

Three types of mechanisms may be referred to collectively as jackhammers; pneumatic, hydraulic, and electromechanical jackhammers. These mechanisms all use similar energy transfers between a hammer and chisel, however they differ in the actuation of the hammer itself (Pang and Goldsmith, 1992). Nonetheless, the mechanisms are placed into a single category due to their shared methods of energy transfer between the internal hammer, the chisel and the impacted material. Demolition breakers are referred to as larger mechanisms exerting high impact energy at lower impact frequencies. Electromechanical hammers are most commonly handheld with low impact energy, while hydraulic demolition breakers are machine mounted and exert high impact energy (Hilti, 2019; Caterpillar, 2019). Handheld electromechanical machines range from 7.5 to 65 J of impact energy (Hilti, 2019) where hydraulic breakers are capable of exerting over 16.27 kJ of impact energy (Caterpillar, 2019).

Pneumatic jackhammers depend on many forms of energy transfer to complete the task of fracturing concrete (Pang and Goldsmith, 1992). Compressed air is used to accelerate the piston towards the chisel. When the piston has contacted the chisel and has transferred its kinetic energy, the air flow is reversed returning the piston to its original position (Figure 2.3.3).

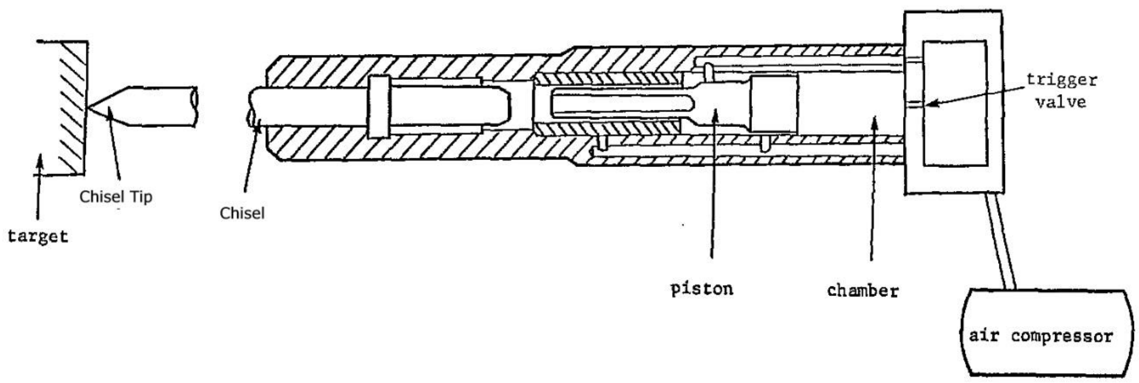

Figure 2.3.3 Primary components of a pneumatic jackhammer (Pang and Goldsmith, 1992)

The energy transferred to the chisel tip is determined by the velocity and mass of the piston within the chamber at the time of collision with the chisel (Pang and Goldsmith, 1992). An energy wave is propagated at the head of the chisel due to the collision of the piston with the chisel, this wave travels through the chisel to its tip. Next, the energy is transferred into the target material and a secondary wave is reflected back into the chisel (Pang and Goldsmith, 1992). When the size of the piston or the system pressure is increased, resulting in high kinetic energy transferred to the chisel (Pang and Goldsmith, 1992). Therefore, the energy transferred to the target material, or impact energy, is increased.

Electro mechanical hammers employ the same energy transfer process between the piston, chisel, and target. In contrast, they implement another method of actuation to accelerate the piston itself. Instead of increasing the pressure within the chamber using compressed air, a secondary piston is moved via an electric motor (Appendix B). The two pistons are separated by an air cushion between them to limit the vibration transferred from chisel impact to the secondary piston assembly. Electro mechanical hammers have a direct relationship between the impact frequency and motor rotation, allowing for direct increase or decrease of impact frequency dependent on the rotational input speed.

Electro mechanical hammers require additional moving components when compared to pneumatic machines. Due to simplification of design and their intense energy requirements, pneumatic and hydraulic hammers are far more capable of providing high impact energy than electro mechanical hammers (Abudayyeh et al., 1998). Electro mechanical hammers are fully enclosed and do not require large machinery to provide power, such as a compressor or hydraulic system (Hilti, 2019). As a result, these hammers are commonly used in hand held applications where electricity is available.

Many downsides also present themselves when jackhammers are used in an urban centre. High energy impacts can induce vibration within structures resulting in unwanted noise and distraction to the everyday lives of people surrounding the site. Modern jackhammers are capable of an impact frequency of 12 to 53 Hz depending on the energy of impact (Hilti, 2019). Energy of impact is dependent upon the force striking the chisel. This energy can range from 7.5 J on small handheld machines to more than 16.27 kJ on large hydraulic machines (Hilti, 2019; Caterpillar, 2019). Larger machines provide higher impact energy at lower frequencies due to mechanical limitations of their design.

2.4 Crack Propagation

During the demolition process, fractures are induced within the material until it can be removed from the structure. High impact energy induces crack propagation, but the initiation of these cracks typically occurs prior to the impact (Guo, 2014). During the curing process of concrete, the mortar and aggregate reduce in size due to dehydration. As the two components do not have the same material properties, they do not dry at the same rate. The reduction in volume of the mortar while curing is greater than that of the aggregate, resulting in micro-cracks at the boundary between the two materials (Guo, 2014). The zone between the aggregate and cement matrix is known as the interfacial transition zone. This zone has 33% to 67% of the matrix tensile strength (Liao, Chang, Peng, and Yang, 2004). As stress in the material increases, these micro-cracks begin to grow slowly, resulting in a weaker and less resilient structure. When 65% of the

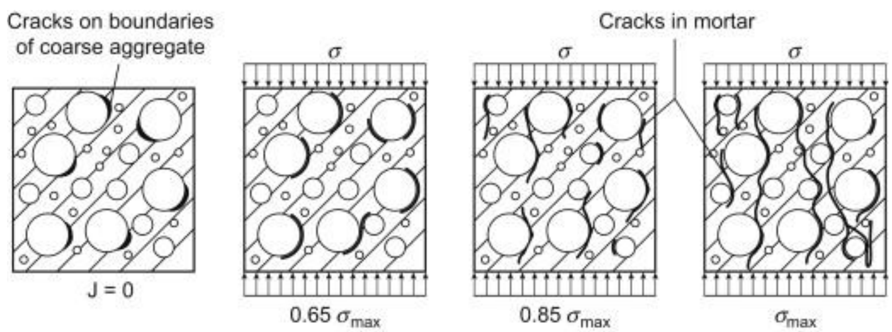

Figure 2.4.1 Crack propagation in concrete (Guo, 2014)

material's maximum stress has been reached, the crack begins to advance along the boundary of the aggregate. Once the stress reaches 85% of its maximum stress, the crack begins to bridge between pieces of aggregate (Figure 2.4.1). Cracks begin to propagate resulting in the hysteretic properties of the material. Stresses induced by sensing or low amplitude vibrations of non-destructive testing can attain 65% of maximum stress (Blitz and Simpson, 1996).

The nature of the material matrix in concrete can induce or resist crack propagation, depending on how the force has been applied to the material and the placement of aggregate material. Dynamic and static load testing of concrete result in different fracture patterns within the material (Chen, Ge, Zhou, and Wu, 2017). High speed impacts result in increased fracture of the material due to higher energy dissipation and increased crack concentration. To illustrate this point, a Brazilian disk was placed within a split Hopkins pressure bar experiment and was tested under high velocity impact, as well as static loading high velocity impact. This resulted in an increased fracture area and indirect crack propagation (Chen, Ge, Zhou, and Wu, 2017).

As time progresses, minerals and chemicals deteriorate the bonds between mortar and aggregate in the material. Oxidization induces the expansion of the re-bar, while placing internal stresses on the material (Hua-Peng, Chen and Nan, 2012). If not properly monitored, these circumstances can lead to material degradation and result in a structure that is no longer stable. Although rarely implemented, the structures can be monitored from within the material by placing strain sensors on the rebar during the construction process. Non-destructive testing is often used to determine the properties of the material based on wave propagation from a point source excitation.

2.5 Crushing and Chipping During Demolition

When an object is struck or impacted by another, the two objects involved in the collision undergo internal stresses and strains due to the change in momentum and the dissipation of energy. Deformation or fracture occurs due to the internal stresses and strains exceeding the yield strength of the material itself.

Benjumea and Sikarskie, in 1969, developed a model for brittle wedge indentation, which showed a crushing and chipping sequence. When a chisel in contact with an isotropic material is struck and results in fracture of the target, two processes occur in sequence. The first process is crushing, which is then followed by a chipping action that removes a second, larger, piece of material (Benjumea and Sikarskie, 1969). These processes are due to the dissipation of the striking energy within the material. Crushing is the inelastic deformation of the material near the chisel. Chipping is due to the secondary tensile forces within the material. Chipping results in the removal of a larger piece of material as a result of the initiation and propagation of cracks in the material (Che, Zhu and Ehmann, 2016).

If sufficient energy has been transferred through the chisel, three zones become apparent post impact. The smallest is the crushed zone, located at the chisel material interface. This zone is composed of a powder-like material that forms following the complete fracture or disintegration of the material. The second zone, the minor crack zone, consists of many tensile fissures shorter than 2mm (Pang and Goldsmith, 1990). These cracks extend in radial directions, demonstrating that their propagation is due to tensile or shear stresses. Finally, the major crack zone encompasses the minor crack zone and consists of a similar style of crack propagation as the inferior zone (Figure 2.5.1). The greatest difference between the two zones is that the length of the crack is longer than 2mm in the major crack zone (Pang and Goldsmith, 1990). When the minor and major crack zones create chips in concrete material, it is due to the overlapping of cracks from individual propagation paths.

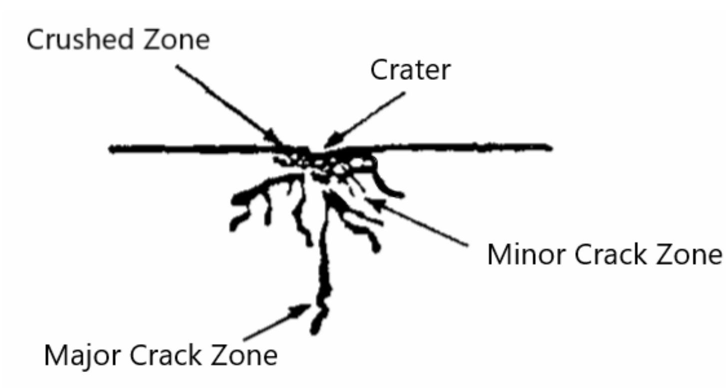

Figure 2.5.1 Characteristic of the crushed, minor crack, and major crack zones. (Pang, and Goldsmith, 1990)

These processes are similar for other brittle materials such as granite and limestone (Pang et al., 1989). Variables such as material characteristics and bedding plane orientation modify the chipping, crushing depth, and protrusion angles seen post impact (Benjumea and Sikarskie, 1969). The geometry of the chip and energy applied during impact can be used to determine the specific energy of the material. Specific energy of the material, in this case, refers to the energy necessary to remove a given unit volume.

The specific energy of the same material can vary greatly depending on the orientation of the bedding plane to the impacted chisel (Wang and Su, 2019). When the bedding angle is 0, or the plane of sedimentation is perpendicular to the axis of impact, the specific energy is minimized

(Benjumea and Sikarskie, 1969). Within concrete there is no discernable bedding plane as aggregate and mortar are distributed randomly throughout the material during the forming process (Guo, 2014).

The crushing and chipping process has been studied and depends greatly upon the material properties, as well as the geometry of the chisel itself. Benjumea and Sikarskie developed the model for rigid wedge indentation in 1969 that was continued by Miller and Sikarskie to model the indentation of truncated and non-truncated conical chisels (Miller and Sikarskie, 1968). This research was then further developed by Pang and Goldsmith in 1989, when a more precise quasi-static force indentation relation for the loading of brittle rocks was created. This provided a more in depth understanding of the force indentation relation during successive cycles. The repetition of the crushing and chipping action is shown, as the force of impact is increased (Figure 2.5.2). The depth of penetration continues to increase during the chipping process, despite the applied force reducing between points H1 and D1 (Pang et al., 1989). This new model more accurately predicts the upper bound of chipping, when compared to the original studies done by Benjumea and Sikarskie (1969).

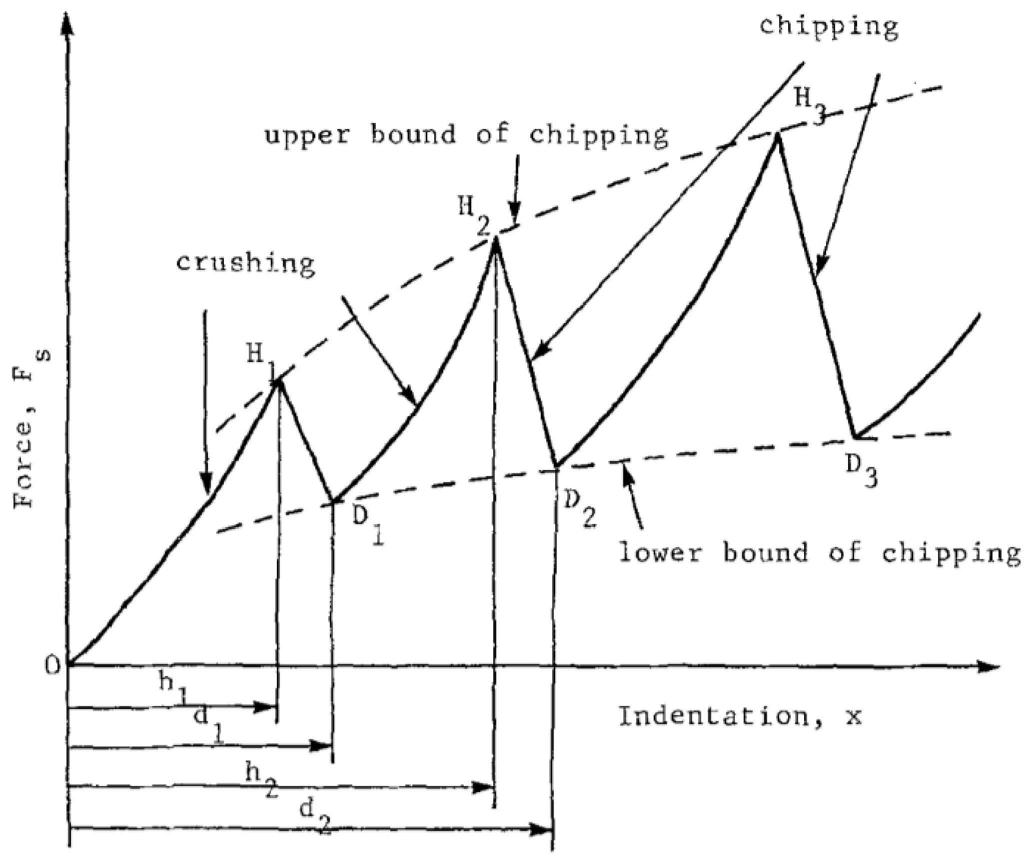

Figure 2.5.2 Indentation graph showing the upper and lower bound of the crushing and chipping process. Despite decreasing force indentation continues to increase during the chipping process. (Pang, Goldsmith and Hood, 1989)

Despite research having been conducted on the chipping process of rock, it has not been concluded whether the chipping process is due to tensile or shear forces within the material (Che et al., 2016). It is currently known that the chipping process requires less energy per unit volume of material removed and therefore provides higher efficiency removal of material (Pang et al., 1989). The size of the crushed zone is relatively small with respect to the chipped zone (Figure 2.5.3). Many of the angles represented in this schematic are dependent upon the angle of the wedge, as well as the properties of the material being impacted. In 1972, Dutta modeled the geometry of the crushing and chipping process and confirmed this model through experimental analysis (Figure 2.5.3).

Due to their inherent complexity, simplification of the processes is necessary to sufficiently create a model for them. These models often make the assumption that there is no relationship between the impact frequency and the crushing and chipping process. An identical jackhammer that is running at 30 or 75 impacts per second will result in the same indentation characteristics, as long as the cumulative number of impacts remains the same. Furthermore, the hammer running at 75 impacts per second would increase the indentation by as much as 2.5 times in the same period when compared to a hammer running at 30 impacts per second.

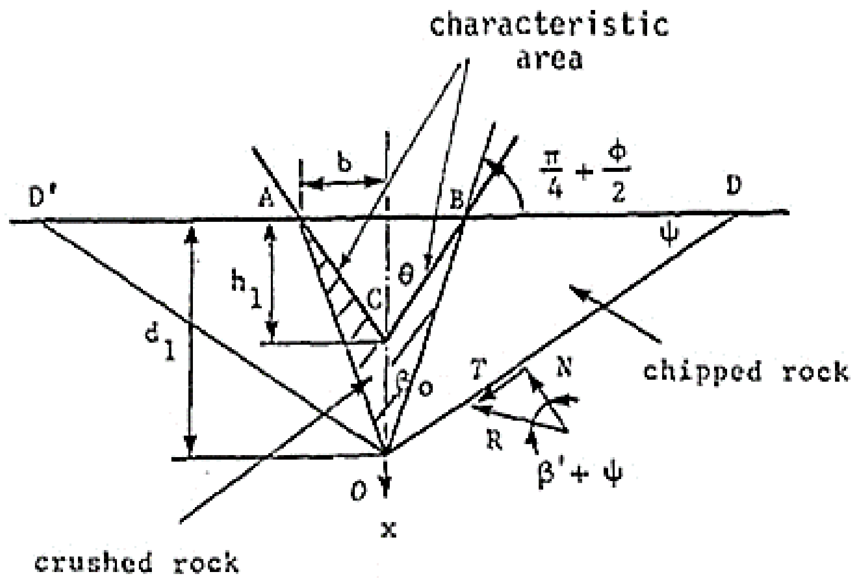

Figure 2.5.3 Mathematical model of the first impact resulting in formation of the crushed and chipped zones. (Dutta, 1972; Pang, 1987)

2.6 Operator Fatigue and Chronic Conditions

Demolition hammers and jackhammers cause the most harm to those who are operating them daily over an extended period. In 1929, Holtzmann began to document the development of degenerative arthritis in workers who used hand held demolition breakers (Fam and Kolin, 1986). Fam and Kolin determined that the operation of a jackhammer may accentuate the tendency of an operator to develop osteoarthritis in their elbows and metacarpophalangeal joints (Fam and Kolin, 1986). The reciprocating action of the internal piston coupled with the intense vibration of the machine itself can deteriorate joint structure and even cause internal organ issues. Shields and Chase investigated a case in 1988 where the patient complained of severe abdominal pain. The patient was a long-term operator of a jackhammer and had operated a heavier machine prior to feeling pain. Upon investigation, it was found that the operator of the machine had sustained a severe torsion of the omentum, a tissue that drapes over the intestines inside the abdomen (Shields and Chase, 1988).

Operator fatigue and hearing loss are both of concern when operating demolition machinery. Jackhammer noise can peak at 118 dBA and has been reported to cause long term hearing loss (Sataloff, Sataloff, Menduke, Yerg, and Gore, 1984). By reducing the impact energy and vibration the operators are exposed to, it may be possible to lower the extreme nature of their working environment and increase the demolition rate.

3 Design of a High Frequency Hydraulic Mechanical Jackhammer

3.1 General Design Criteria

The modern jackhammer has many technological deficiencies. To innovate based on current knowledge and technological advancement, a modified jackhammer system was designed. Previous research assumes that the mechanics of multiple impacts can be modeled as a repetition of a single impact (Benjumea and Sikarskie, 1969; Pang et al., 1989). Impact frequency is not taken into consideration in the mathematical models developed by Pang and Goldsmith in 1989.

In accordance with this premise, an increase in impact frequency would result in an increase in material removal per unit time. A jackhammer that is operating at twice the impact frequency should be capable of removing roughly twice the material as another hammer over the same period. This would correlate with the specific energy of the concrete itself. If there is a given energy per unit volume of material that is removed from the structure, increasing the impact frequency will result in an increase in the energy applied to the concrete, as well as increase the rate at which the material is removed.

A machine was designed that was capable of reaching impact frequencies exceeding 75Hz, while remaining of manageable size to operate for testing purposes. This initial design was based on proof of concept to validate the hypothesis, it was not meant to be a commercially viable machine.

Acoustic, electromagnetic, and oscillating mechanisms were investigated for their ability to reliably reach high frequencies. To minimize the variation in the transfer of impact energy into the material, the mechanism that transfers the impact energy to the concrete must remain unchanged. The impact between an internal hammer and the chisel would not be replicated within these mechanisms resulting in a variation of energy transfer. Electro-mechanical, hydraulic, and pneumatic demolition hammers all implement a reciprocating hammer that strikes a chisel. The mechanical design of a hammer striking a chisel was to be replicated. Due to the internal complexity of these mechanisms, the integration of a commercially available mechanism allowed for simplified fabrication.

The size of the hammer was to remain manageable to facilitate testing and reduce fabrication costs. The hammer must be large enough to exert enough impact energy to induce a crushing cycle. Small rotary demolition hammers were not considered due to their low impact energy. The internal mechanisms of handheld commercially available hammers exerting 20 J to 35 J of maximum impact energy were considered for this design.

3.2 Machine Design

Commercially available hammers cannot meet the experimental requirements as they do not reach the required impact frequencies. Typical hammers operate at an impact frequency of 32.5 Hz (Hilti, 2019). A high-frequency dual head hydraulic mechanical jackhammer was fabricated to allow high frequency demolition without pushing a single unit to failure. This design process was taken on for the sole purpose of generating preliminary test data. Long term operation and reliability was not considered in this design and a failure model was not developed. The design placed two electro-mechanical jackhammers in parallel, operating in alternating sequence. The electric drive portion of the electro-mechanical hammer was modified to be powered via a hydraulic motor. The two hammers were designed to receive a single "Y" shaped chisel (Appendix A). This chisel was custom designed and built for this application. The chisel enables two hammer mechanisms to operate in alternating sequence, while transferring energy to a single chisel tip. This tip received equivalent impact energy from both mechanisms, as the system is symmetrical. When the two mechanical heads are perfectly out of time, the synergistic actions of both mechanisms result in the production of elevated, uniform, impact frequency. Essentially, this chisel design allows for two individual mechanisms to operate at 35 Hz while providing an impact frequency of 70 Hz. This multi-hammer design requires supporting machinery to maneuver and place the system for demolition. Future designs will focus on the ergonomics and integration into the construction site.

To reduce variation in energy transfer, existing hammers were reconfigured to meet the design requirements. The Ironton Demolition Breaker, model 46479 (Appendix B), was used as the basic hammer and modified to achieve the research goal. This machine has an impact energy of 25 J and a maximum impact frequency of 1800 BPM or 30 Hz. The chuck was designed to receive the industry standard Slotted Drive System (SDS) Max chisels (Wache, 1999). The machine was originally powered by an electric motor equipped with a variable drive with a maximum rotation of 15,000 RPM. It was not possible to run the electronic drives of these machines in sequence without modification.

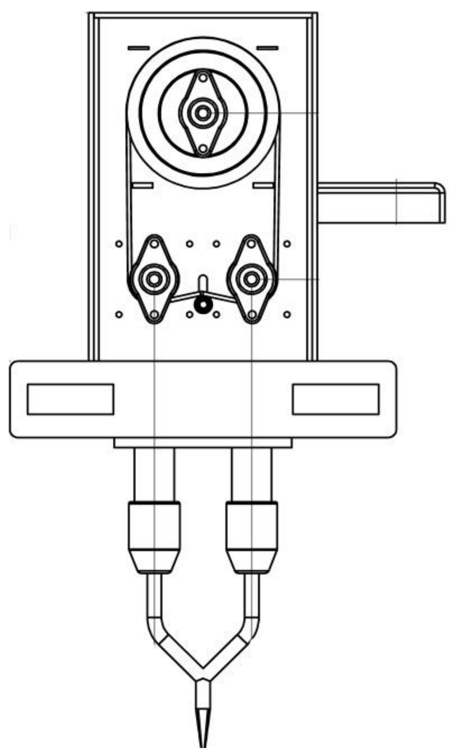

Figure 3.2.1 Preliminary design showing the pulley system, two receiving heads, and "Y" shaped chisel.

To maintain a constant impact frequency without deviation, the input shafts were mechanically connected via a timing belt. When one piston is located at top dead centre, the other must be at bottom dead centre to ensure that the impact frequency is in alternating sequence and not an off-beat variation (Figure 3.2.1).

The input shaft was fabricated from the main motor shaft. The rotor and fan, parts 34 and 35 (Appendix B), were removed from the motor shaft. The motor shaft was repurposed as an input shaft with the stock helical gear connecting into part 44 or the main drive gear. The input shaft and the main drive gear have a ratio of 8.5:1. To achieve an impact frequency of 75 Hz or a single mechanism impact frequency of 37.5 Hz, the input shafts must rotate at 19,125 RPM. The fundamental design requirement of this hammer was to attain a 75 Hz impact frequency.

A timing belt and sprocket system was designed for the secondary stage power transmission. A ratio of the driving sprocket to the driven sprocket was 1:3.32. The driving sprocket was connected to the driven gear of the primary gearbox that ultimately connects to the motor. This gearbox is a Flowfit 1:3.8 ratio box and contains two conventional parallel axis spur gears. The construction diagram for this gearbox is shown in Appendix C. The entire drivetrain of the jackhammer from the motor to the input shaft of the hammer mechanism (Figure 3.2.2).

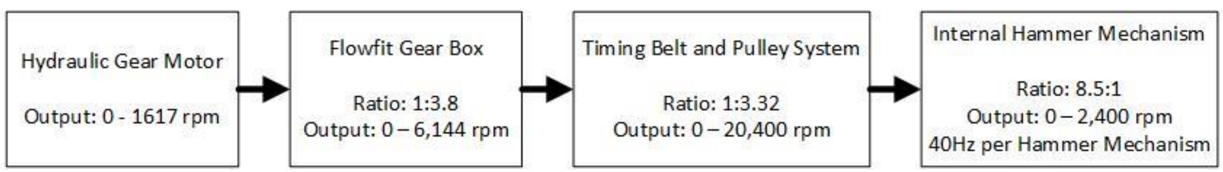

Figure 3.2.2 Drivetrain representation from input power at the hydraulic gear motor to the internal hammer mechanisms.

To achieve an impact frequency of 75Hz, the primary input shaft, must revolve at 1,489 RPM. Due to inefficiencies within the timing sprocket and gearbox, this machine required a motor with high starting torque and a maximum output shaft rotation of at least 2834 RPM. The hydraulic gear motor used was rated at 23.8 LPM consumption, 18 MPa at 3600 RPM. A hydraulic gear motor was used to drive the jackhammer as it provided high torque at start-up and was compact when compared to electrical or pneumatic motors. In addition, hydraulic power sources were readily available at all testing locations.

3.3 Chisel Fabrication

A chisel design was required to connect the hammer mechanisms together and transfer the impact energy to a single tip, where it would then be transferred to the material. The internal hammer, or “ram”, (part 22, Appendix B) impacts the head of the chisel. This impact surface must remain unchanged, as modification would alter the energy transfer from the hammer to the chisel. The chisel was fabricated from two commercially available SDS demolition chisels. These chisels were re-designed to transfer energy in a uniform manner from both heads to a single tip.

A “Y” template was configured, as shown in appendix A, to receive both hammer mechanisms while transferring energy to a single tip. Two chisels were cut, bent, and welded together to form the upper dual head section, while a single tip was used for the lower portion. Chisels with two different tip designs were utilized during testing. A moil point chisel was used for preliminary testing and a cold chisel was used for secondary testing. The cold chisel was fabricated and tested after the first test sequence was completed with the moil point chisel to further investigate the effects of tip geometry on deterioration pattern.

3.4 Control Components

The machine was designed to operate at high speed, it is required to manipulate the rotational speed of the motor accordingly. A “soft start” was required to allow the driveline time to gradually work its way up to full operating speed. A flow regulator was used between the hydraulic pump and motor to divert the flow during the start sequence. The hydraulic flow diagram is shown in Appendix D.

The machine was timed by opening the top cover, part 50, of the first hammer mechanism and rotating the input shaft until the connecting rod, part 30, was at bottom dead center. The position of the input shaft was then recorded. This process was repeated with the second hammer mechanism placing the connecting rod at the top dead center or 180 degrees out of sync of the first hammer. When both mechanisms were placed in the correct position, the timing belt was installed. The installation of the timing belt connects the two shafts ensuring that they operate in unison.

3.5 Mechanical Design Specifications

The mechanical components of the machine were assembled to meet the short term testing parameters and allow for preliminary testing. The foundation of the design was to operate two pre-fabricated hammers in parallel, the following components were assembled to power such a system. Mechanical components of the machine are as listed;

- Driving Timing Pulley: 183.35mm diameter, 72 tooth – P72-8M-20FP
- Driven Timing Pulley: 56.02mm diameter, 22 tooth – P22-8M-20F
- Timing Belt: 8mm wide, 920mm long, 20mm pitch
- Drive Shaft and Idler Shaft Self Aligning Bearings: 12 mm internal diameter flange mounted, HCFL201
- Hydraulic Motor: Haldex, Serial Number: 1820068 RPM range 300-3000 RPM.
- Flow Control Valve: Prince Hydraulic Compensated Flow Control RD-175-30 .75”

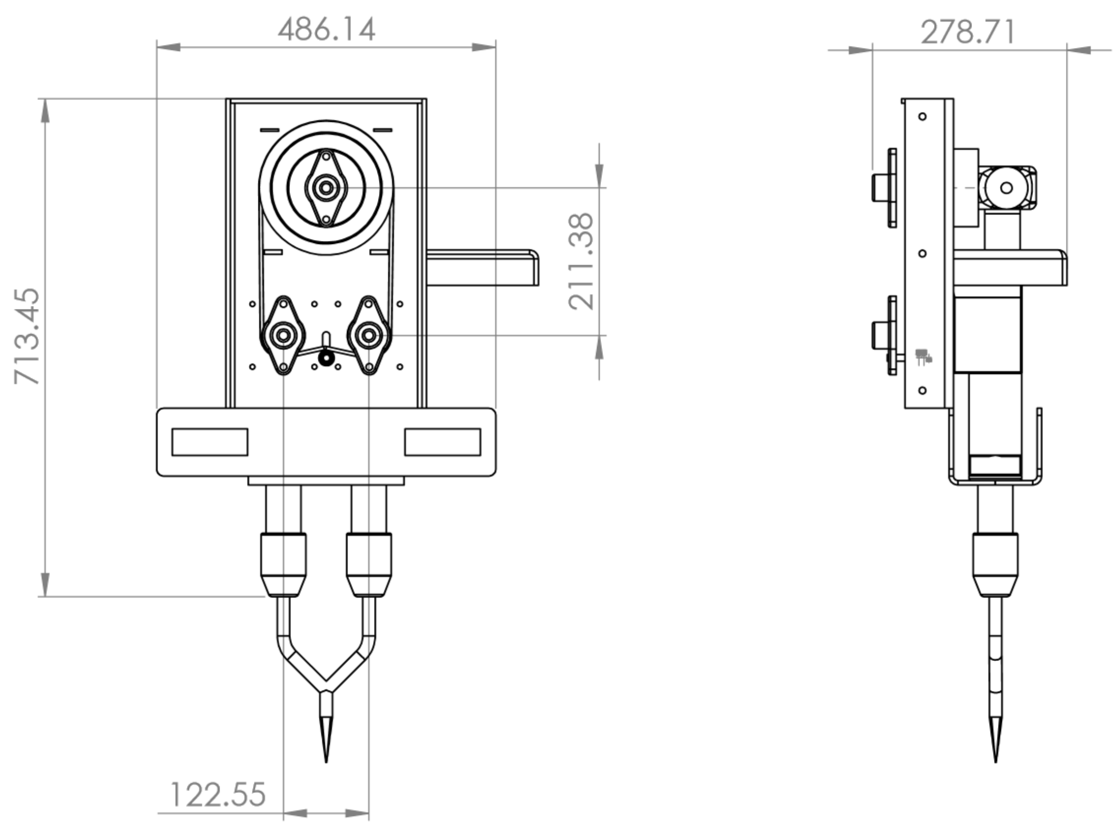

Figure 3.6.1 Front view of the hydraulic mechanical jackhammer as designed in Solidworks™. All measurements are in mm.

3.6 Final Design and Fabrication

The machine was designed using the computer assisted design software, Solidworks™ (Figure 3.6.1). Any components that required computer assisted fabrication were sent out to a third party. Jackhammer mechanism input shafts were salvaged from the Ironton jackhammers and re-used. The two driven shafts are directly aligned with the chisel head and hammer mechanism (Figure 3.6.1). The large pulley is the driving pulley and the two smaller pulleys are the driven pulleys (Figure 3.6.2). The two driven pulley shafts were timed before placing the belt as outlined in Section 4.2.2.

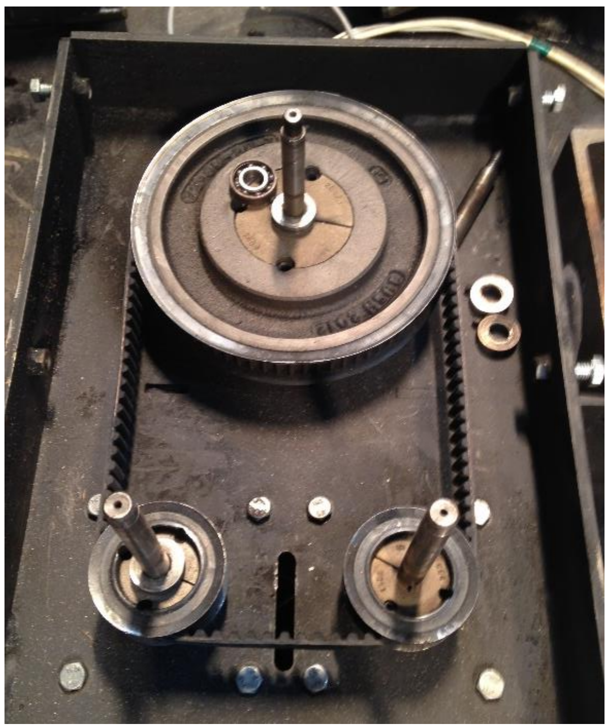

Figure 3.6.2 Timing pulley system with belt installed and face plate removed.

4 Proof of Concept Testing

4.1 Introduction

The following testing methods were developed to determine the functionality of a dual head hydraulic mechanical jackhammer. The machine itself was designed for short periods of operation and to provide clarity on the effectiveness of the fundamental design. A testing sequence was developed and completed. Some limitations due of the mechanical design were apparent, although these limitations did not prove to be barriers.

4.2 Methods and Materials

The methods used in this testing procedure were designed with the goal of proving the functionality of a dual head jackhammer design, while attaining high frequency impact and using a single tipped chisel. Functionality was determined by inspection of the impact location after the test sequence was completed. An analysis of the audio recording was also completed, in order to confirm if impact frequency was indeed attained. The preparation and testing processes were done in three distinct steps; slab preparation, machinery setup, and impact sequence testing.

4.2.1 Slab Preparation

Three individual testing slabs were poured to provide a uniform, non-reinforced, unaltered surface to minimize variation within the test material. The dimensions of each slab were 70 cm long, 70 cm wide, and 30 cm high. Concrete used for the slab was Quikrete concrete mix product number 1101 (Quikrete, Atlanta GA. United States). Compressive strength of this mixture is rated at 27.6 MPa as per ASTM C39. A pre-mixed product was used to minimize variation in aggregate size and distribution. The entire slab was poured at once and allowed to cure in a controlled environment as per the manufacturer's guidelines. The slab was cured for a minimum of 28 days before preliminary testing and more than 56 days before high frequency testing. The slabs were not subject to freeze thaw cycles and were stored in a controlled environment between 18°C and 23°C.

Materials

- 26 bags of Quikrete 1101 concrete mix, 27.2kg per bag
- Concrete mixer, minimum capacity of 125l (minimum of 1 slab)
- Trowel
- Shovel
- 20 L measuring vessel
- 1 L vessel
- Clean water source

4.2.2 Machinery Setup

The pre-start procedure was followed to ensure that the jackhammer was setup in a safe and functional manner. Hydraulic fluid at high pressure and shafts rotating at high speeds present high risk of injury if not operated with caution.

1. The jackhammer was securely mounted on a lifting device to provide vertical and horizontal adjustment. A manually operated hydraulic fork lift was used for this test.

2. The chisel was installed by pushing upwards on the tool retention head or part 9, Appendix B. Both tool retention heads were pushed upward simultaneously, and the moil point chisel was inserted. The lift was then moved to place the tip of the chisel over the test slab. The tip was placed no less than 10 cm from the edges of the slab to avoid stress concentrations along the edges.
3. The jackhammer was then loaded with ballast weight to provide downforce during testing. A total of five weights were mounted on either side of the hammer providing a total ballast weight of 34 kg. The ballast weights were secured tightly to the jackhammer using the large C-clamps and the jackhammer was then secured to the lifting device using the ratchet straps.

4. The jackhammer required power from an external hydraulic system. The jackhammer's hydraulic system, outlined in Appendix D, has two male 0.5 inch hydraulic coupling tips that will mate with any 0.5 inch ISO 5675 female outlet. A New Holland T5060 was used as a power source as it provided reliable hydraulic pressure and flow. Any machine that can provide 37.8 L min^{-1} at 18 MPa may be used as a power source.
5. Before any lines were connected to the power source, the hydraulic system was inspected for line breaks, leaks, and unusual wear. The systems on the power source were reviewed to ensure that the high- and low-pressure outlets were properly labelled. The hydraulic couplings were then securely connected. A visual and audio recording was taken during testing. The audio portion of this recording was then used to determine the precise impacts per minute that was reached. Camera distance, and location were not imperative

Figure 4.2.1 Jackhammer installed on lifting device with ballast and chisel prepared for testing.

and were dependent on both view and allowing a safe working distance around the machinery.

Materials

- Hydraulic Mechanical Jackhammer as described in Chapter 3.
    - Moil Point Chisel, Appendix A
    - Cold Chisel, Appendix A
- Testing Slab
- Rigid 18 volt portable drill with .0625 inch socket
- 2 Ratchet Straps
- 2 Large C Clamps
- New Holland T5060 (or equivalent machine capable of providing a minimum of 37.8 L min^{-1} at 18 MPa of hydraulic flow.
- Canon EOS T4I digital SLR Camera
- Hydraulic fork lift (capable of lifting a minimum of 100 kg)

4.2.3 Impact Sequence Testing

Before starting any of the machinery involved with testing, a final inspection of all components was completed. All components were shown to have been installed correctly and the machinery was proven to be safe for operation. Succeeding this final check, the following steps were performed:

The camera was turned on and a video recording of the proceeding test sequence began. The tractor's engine was started, and the hydraulic implement lever was engaged. Hydraulic fluid began flowing through the flow regulator and directly back to the low-pressure return. No hydraulic pressure was placed on the jackhammer's motor at this point.

The drill with a 0.625 inch nut driver was mated with the 0.625 inch nut threaded onto the driving pulley shaft. The drill was engaged, and the shaft began spinning in a clockwise rotation. The maximum rotation of the drill was reached at 300 RPM. 300 RPM was maintained until the hydraulic motor surpassed the speed of the drill. This step was necessary to reduce the starting torque placed on the hydraulic motor.

The hydraulic flow regulator valve was then slowly increased to 25% maximum throttle over a period of 15 s. At this point, the hydraulic motor began to power the jackhammer. The driven pulley's rotational speed quickly surpassed 300 RPM. The connection between the drill and the driven pulley shaft was removed due to the shaft spinning faster than the threaded bolt.

As the hydraulic flow regulator valve was slowly increased to 50% maximum throttle, the machine began to reach operating speed over a period of 15 s. When the machine reached maximum rotational speed at this throttle setting, the tip was lowered onto the concrete slab. This was done by lowering the hydraulic lift until the full weight of the hammer rested on the tip.

The moment the jackhammer's weight was placed on the tip, the chisel was automatically engaged, and material demolition began. The tip was allowed to penetrate into the material until it no longer advanced into the material. It was then lifted using the hydraulic lift and repositioned to another unaffected location on the slab.

When the tip was positioned over an unaffected portion of the concrete slab, it was lowered once again and allowed to penetrate until it remained stationary. This process was repeated three times and the tip was then raised. The hydraulic flow regulator valve was slowly increased to 75% throttle over a period of 15 s. The process of lowering and raising the jackhammer three times was then repeated on an unaffected piece of concrete.

The tip was then raised, and the hydraulic flow regulator was reduced to 0% throttle over a period of 30 s. The machine was then allowed to reduce speed until it was at rest and the moil point chisel could be removed. The cold chisel was then inserted into the retention head and the process of starting up, reaching operating speed, lowering and raising the jackhammer was repeated.

After the test was complete, visual observation of the indentations were recorded before and after being cleaned with compressed air.

4.3 Results

4.3.1 Impact Frequency Analysis

Impact frequency was determined by analyzing the audio recording of each impact sequence during the test. The audio file was slowed down to 0.025% of its original speed and the impacts per second were counted. Audio analysis was completed using the software Audacity®. The number of impacts was then cross referenced with the number of periodic increases in the audio file frequency graph. Each audible impact clearly corresponded to an increase in the frequency graph (Figure 4.3.1). For a 0.2 s sample time, at 50% throttle, the frequency graph showed 11 periodic increases in signal intensity. This corresponded to an impact frequency of 55 Hz. The impact frequency was calculated toward the beginning, middle, and end of each impact sequence. Each sample was 0.2 s in length. An average of the three samples was taken as a representative value for the impact frequency during the impact sequence. Impact sequences ranged from 4.9 to 5.8 s in duration. Observed impact frequencies are shown (Table 4.3.1) for the moil point chisel, the cold chisel (Tablet 4.3.2).

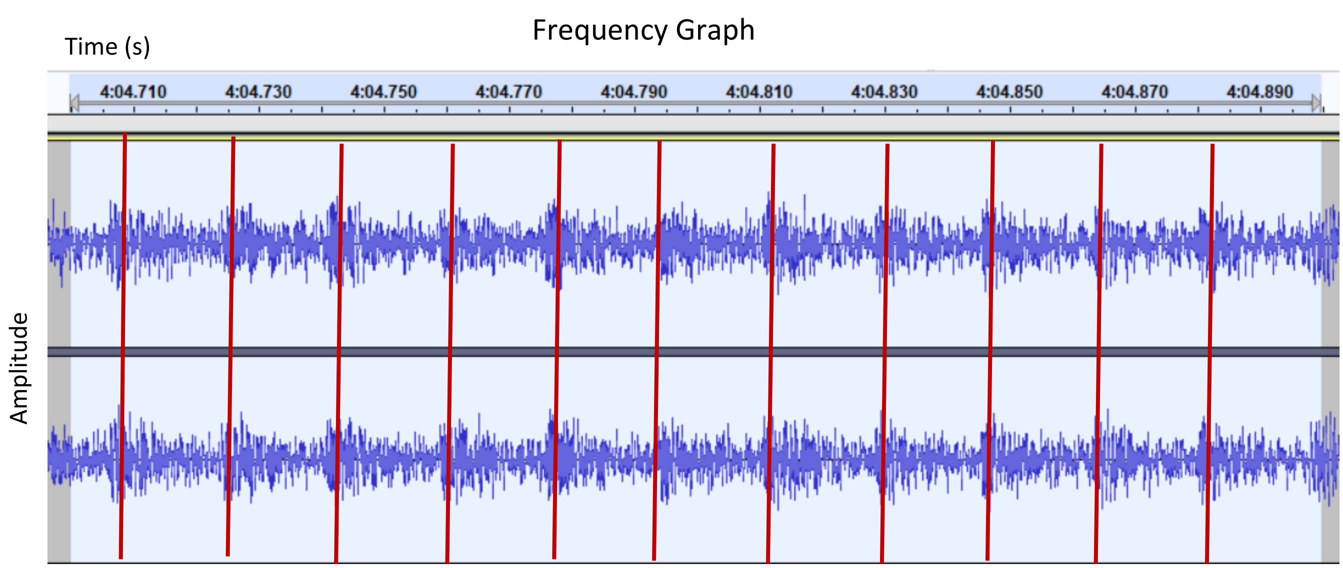

Figure 4.3.1 Audio frequency graph showing a 0.2 s sample of a 4 s impact sequence. Red lines have been added to show the periodic increases representing the hammer impacts. This graph is to visually represent the analysis done by listening to and analyzing the audio recording.

Moil Point Chisel							
Throttle	Impact Period (time stamp)	Time Stamp Start	Time Stamp End	Time Passed (s)	Impacts Counted	Impact Frequency	Average Impact Frequency (Hz)
50%	4:04.7-4:08.0 (4 s)	04:04.7	04:04.9	0.2	11	55	58.3
		04:06.0	04:06.2	0.2	12	60	
		04:07.7	04:07.9	0.2	12	60	
50%	4:11.4-4:17.2 (5.8 s)	04:11.4	04:11.6	0.2	12	60	60.0
		04:14.3	04:14.5	0.2	12	60	
		04:17.0	04:17.2	0.2	12	60	
50%	4:19.8-4:24.9 (5.1 s)	04:19.8	04:20.0	0.2	12	60	58.3
		04:22.3	04:22.5	0.2	11	55	
		04:24.7	04:24.9	0.2	12	60	
75%	4:51.4-4:56.5 (5.1 s)	04:51.4	04:51.6	0.2	16	80	80.0
		04:53.9	04:54.1	0.2	16	80	
		04:56.2	04:56.4	0.2	16	80	

Table 4.3-1 Moil point chisel impact frequency analysis.

Cold Chisel							
Throttle	Impact Period	Time Stamp Start	Time Stamp End	Time Passed (s)	Impacts Counted	Impact Frequency (Hz)	Average Impact Frequency (Hz)
50%	0:03.8 - 0:09.0 (5.2 s)	00:03.8	00:04.0	0.2	11	55	55.0
		00:06.4	00:06.6	0.2	11	55	
		00:08.8	00:09.0	0.2	11	55	
50%	0:10.1-0:15.2 (5.1 s)	00:10.1	00:10.3	0.2	12	60	60.0
		00:12.6	00:12.8	0.2	12	60	
		00:14.9	00:15.1	0.2	12	60	
50%	0:28.3-0:33.5 (5.2 s)	00:28.3	00:28.5	0.2	12	60	58.3
		00:30.8	00:31.0	0.2	12	60	
		00:33.0	00:33.2	0.2	11	55	
75%	0:50.6-0:55.5 (4.9 s)	00:50.9	00:51.1	0.2	17	85	81.7
		00:53.5	00:53.7	0.2	16	80	
		00:54.2	00:54.4	0.2	16	80	

Table 4.3-2 Cold chisel impact frequency analysis.

4.3.2 Material Demolition

All tests showed material demolition as a result of impact energy transfer from the chisel tip into the concrete. By reviewing the video recording of each impact sequence, each hammer provided impact energy to the chisel resulting in material demolition. This was clear as each percussion that was used to determine the impact frequency showed simultaneous material degradation.

The first test was done with the moil point chisel. The residual dust was removed from the indentation and the impact location was visually inspected. All three impact sites showed similar fracture patterns. Chipping was evident at the beginning of the impact sequence but once the chisel had made its way into the material minimal chipping could be seen. This was visualized by the clear-cut shape of the chisel into the concrete. All flat faces of the moil point chisel were clearly visible to the point that the corners remained sharply cut into the concrete (Figure 4.3.2).

Figure 4.3.2 Moil point chisel indentation following a 4 s impact sequence at 55Hz impact frequency.

Red machinists' ink was used to stain the indentation from the 75% throttle, 81.7 Hz test sequence. Penetration was rapid and fine dust remained in the indentation after the sequence was complete. Once cleaned out, the indentation was clear and showed minimal crack propagation into adjacent material. Apart from aggregate that protruded from the path of the chisel, the indentation was uniform. The indentation is visualized using red machinist's ink to show the clear edge and surface of the chisel remaining in the material after the impact sequence (Figure 4.3.3). Lateral chipping or crack propagation was not visible.

Similar results were seen when assessing the visual recording and observations from testing of the cold chisel. The cold chisel rapidly penetrated the material and when removed, left behind an indentation filled with very fine dust and debris. The entire elongated tip of the chisel showed a clean-cut indentation into the material. This impact sequence also demonstrated minimal lateral crack propagation into the material resembling limited initiation of a chipping stage (Figure 4.3.4).

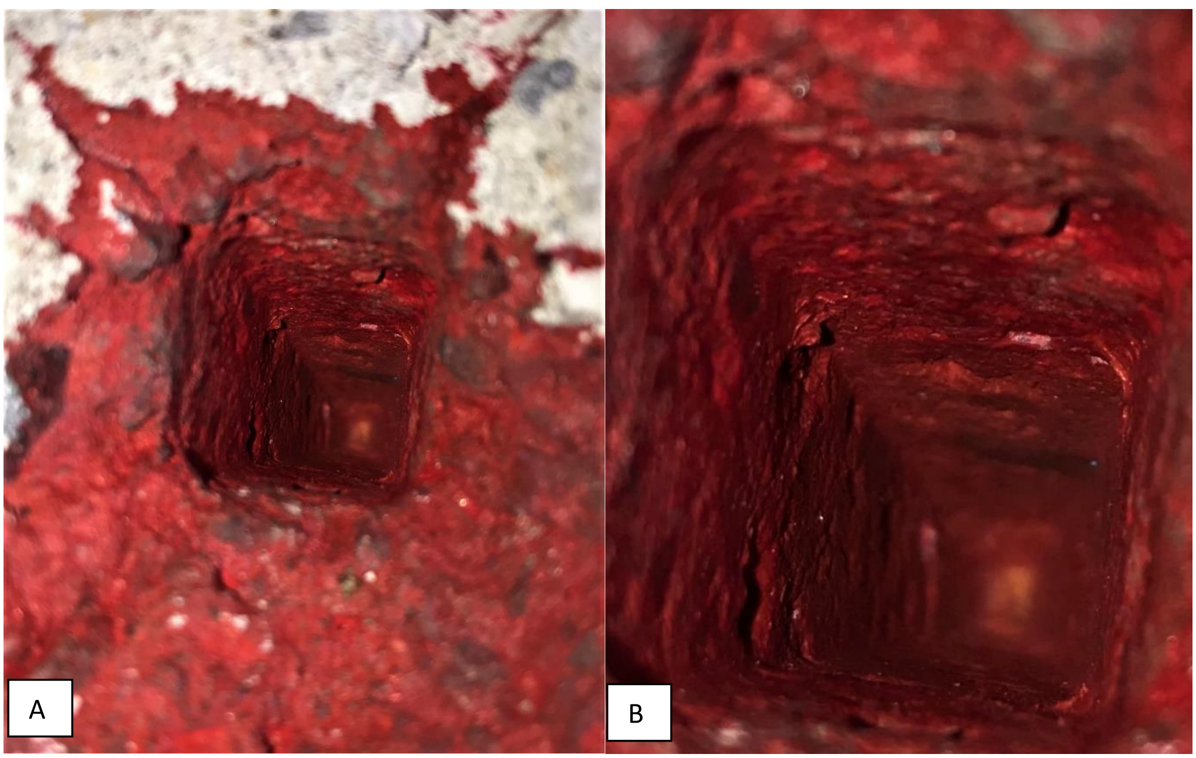

Figure 4.3.3 Moil point chisel indentation following a 5.1 s impact sequence at 80Hz impact frequency. Indentation was died red to show the lack of lateral chipping. A, an overall view and B, showing two distinct protrusions on the left plane where aggregate was removed.

4.4 Discussion

4.4.1 Impact Frequency

The primary objective for this testing sequence was to determine if the newly designed machine could reach impact frequencies in excess of industry standards, and at these frequencies, was demolition observed. Jackhammers of similar impact energy to the Ironton machine, which were used as a foundation for this experiment, are capable of reaching 35 to 40 Hz. From the analysis of the audio recording, shown in Table 4.3-1 and 4.3-2, at 50% throttle on the hydraulic flow regulator, an impact frequency ranging from 55 to 60Hz was attained. At 75% throttle, average impact frequencies during each impact sequence were 80 to 81.7 Hz. Inspection of the impact location after the impact sequence was completed demonstrated that demolition of the material had occurred during each impact period, ranging from 4.0 to 5.8 s (Figure 4.3.2, Figure 4.3.4). The impact frequency analysis associated with the observational data confirmed that the machine ran at upwards of 81.7 Hz and at these elevated frequencies material demolition was achieved.

Figure 4.3.4 Cold chisel indentation following a 4.9 s impact sequence at 81.7 Hz impact frequency.

The multi head chisel design did transfer the impact energy through to the material, as can be seen in the resulting indentation (Figures 4.3.3 and 4.3.4).

By running this machine at 50% and 75% of its maximum capacity, the functionality of the hammer was confirmed. Despite issues seen with the hydraulic system, the mechanical design of the hammer was able to reach the impact frequencies that the machine was designed for. The innovative design implementing two individual hammer mechanisms coupled to a single chisel tip with the goal of increasing impact frequency was confirmed. Currently, there are no jackhammers or demolition hammers available that implement such a design.

Due to the timing of the two individual mechanisms, vibration from the machine was reduced significantly. The linear motion of each internal piston is in the opposite direction at any given moment during operation reducing the oscillation or "hopping" of the hammer itself during operation. Further testing is necessary to quantify the extent of reduction in oscillation and how this correlates to improved operator ergonomics. Despite many fundamental design limitations of the machine used for this preliminary testing, the concept and functionality of the design was confirmed.

4.4.2 Penetration and Chisel Design

Two chisel designs were tested during this experiment; a moil point chisel and a cold chisel (Appendix A). The two chisels represent different tip geometries and inspection of each indentation provided a cross reference for the demolition sustained. Across impact sequences, material indentation remained a clean-cut imprint of the chisel geometry. The imprint of the moil point chisel shows clear cut planes and edges of the pyramid shaped chisel itself (Figure 4.3.3). The cold chisel displays a thin elongated cut pattern with very few irregularities from the geometry of the chisel (Figure 4.3.4). The material that remained in the indentation after the impact sequence consisted of powdered mortar and small aggregate. The only period during testing where large chips were removed from the material was during the first few impacts where fine scaling chips were removed from the surface. After the tip had penetrated the material, only minimal chipping was observed. The geometry of the indentation also suggests that the chipping that was observed was not significant.

4.4.3 Crushing and Chipping

The similarity between the geometry of each indentation demonstrates that the geometry of the chisel did not have a significant impact on the indentation characteristics. Lateral crack propagation should have been visible through its protrusion from the indentation site. This would make the shape of each site irregular, when compared to the shape of the chisel tip itself. The results of these preliminary tests would suggest that the crack propagation during the chipping process is localized. Localized crack propagation or limited demolition of material during the chipping process may occur due to the high frequency of impact.

The crushing and chipping process has two phenomena that occur in sequence following the impact. If another impact is made prior to the completion of the entire sequence, the chipping process may be affected, given that it is the secondary component. The duration of time for the crushing and chipping process is dependent on the material characteristics. Due to the non-homogeneity of the material, this sequence timing can vary during operation.

4.4.4 Limitations on Testing

Due to mechanical deficiencies of the hydraulic system, further testing was not possible with this configuration. Starting torque surpassed the designed stall torque of the hydraulic motor resulting in the premature failure of the motor shaft seal. The testing that was successful has provided enough data to show that the machine is effective in producing a high frequency impact resulting in indentation of the slab material.

The cold point chisel fractured at the weld after the 75% throttle test. Despite having successfully ran the initial test, further testing was not possible. The chisels are composed of high strength, high carbon steel and are not intended to be welded or modified. To accomplish preliminary testing, the fabrication of the chisel was completed to provide a proof of concept. These limitations were not viewed as detrimental to the testing process, however they do provide a starting point for further design improvements.

5 General Summary

A full review of the technology currently available for concrete demolition was completed. Demolition breakers and jackhammers were found to be the most common method of concrete demolition due to their ease of use, high production rate, and their versatility (Abudayyeh et al., 1998). It was found that as the impact energy of a hammer increases, the impact frequency decreases. Small handheld jackhammers have an impact frequency of 15 to 53 Hz (Hilti, 2019) while large hydraulic demolition hammers operate at 11 to 18 Hz (Caterpillar, 2019). Moreover, the higher the impact energy (lower impact frequency) that is exerted by the hammer (Caterpillar, 2019), the louder and more intrusive it is to the machine's operators and neighboring residents.

A new design of jackhammer was developed that implemented multiple hammer mechanisms that are joined by a single, multi-head, chisel. The method of demolition follows traditional practices while modifying the machine's functionality. This design was developed in accordance with research of Pang and Goldsmith that assumes the material crack propagation and indentation models of multiple impacts is not affected by the frequency of impact (Pang et al., 1989). This new design of jackhammer was capable of hitting more often to increase the production rate of the hammer when compared to a hammer of similar impact energy. The destruction specific energy of the concrete represents the energy required to remove a single unit volume of material from the structure (Atici and Ersoy, 2008). By increasing the impact frequency, more energy is being transferred to the material over a shorter period and therefore increasing the quantity of material that is removed per unit time.

The design of a multi-head jackhammer reduces the inertial force of single hammer mechanism moving back and forth. With two or more mechanisms running in parallel and properly timed, these forces were negated within the overall system. This design was a preliminary proof of concept that would determine if it was possible to operate two hammer mechanisms in parallel and still achieve concrete demolition.

A multi-head hydraulic mechanical jackhammer was built for testing purposes. Slabs of 70 cm in width, 70 cm depth, and 30 cm thick were used for the testing process. The hydraulic mechanical jackhammer was tested at 50% and 75% of its maximum capacity reaching 55 and 80 Hz respectively. Concrete indentation was achieved, and preliminary observation would show that a very limited minor and major crack zone was apparent. This suggested that a limited chipping process occurred during testing and thus further testing is required to determine the extent of crack propagation within the material.

5.1 General Conclusion

Many different methods of concrete demolition have been developed for use within the urban landscape. These methods include expansive agents, hydraulic splitting, hydro demolition, as well as hydraulic, pneumatic, or electro-mechanical breakers. Hydraulic demolition hammers and jackhammers have remained a standard in the demolition and removal of material within the construction industry. Despite having been developed in 1894, the modern-day jackhammer remains somewhat antiquated (King, 1894).

The functionality of a dual head jackhammer with a single tip chisel was confirmed and impact frequencies of over 80 Hz were attained. These results are more than 2.4 times the industry standard of 32.4 Hz. Through careful observation during the testing process, material demolition was found to occur (Figure 4.3.1). The rate of material demolition was reduced, as the indentation was filled with fine powder and debris from the material itself. This powder acted as a buffer between the chisel and the material, absorbing the impact energy and limiting fracture. Chisel geometry did not show considerable variation in indentation characteristics. Analysis of the indentation characteristics is necessary to determine the extent of the chipping process that has occurred within the material in proximity to the impact location.

This research demonstrated that a two headed hydraulic mechanical jackhammer equipped with a dual head, single tipped, chisel can reach an impact frequency of 80 Hz. This jackhammer exerted an impact energy of 25 J and originally 30 Hz. This equated to a total of 750 W of energy exerted toward material demolition. With the same impact energy of 25 J at a frequency of 80Hz equates to a total of 2 kW of energy exerted toward demolition.

This preliminary design verification may be a step toward the development of high frequency demolition. This new method of demolition will not drastically change the act of removing concrete from a procedural perspective. Despite the requirement of similar machinery and supporting equipment, high frequency demolition of material will focus on increasing the impact frequency before increasing the impact energy. This change in mentality will not only improve the lives of workers who use demolition equipment but will also reduce the impact that their equipment has on neighboring communities.

5.2 Further Suggested Studies

Further research is required to understand the extent of the crushed, minor crack, and major crack zones within the material when impacted at frequencies of more than 75 Hz. This research should follow the methods outlined by Pang and Goldsmith in 1990 when examining the response of elastic and brittle targets to loading by a conical and wedge type chisel. This will provide precise cross-sectional analysis of the indentation to show a crack propagation pattern. These patterns must be referenced with the work done by Dutta in 1971 to determine if the crushing and chipping zones are properly predicted within the models. If the models are accurate, it would suggest that an increase in impact frequency will correlate directly to an increase in material removal. This would also suggest that an efficient way to increase the demolition rate of any hammer would be to increase its impact frequency.

Finally, an analysis of the destructive specific energy of the test material must be done, along with a full analysis of the energy transfer within the mechanism. This assessment would be focused on determining if an increase in energy exerted toward demolition correlates to an increase in material removal. This research would demonstrate the potential of a linear relationship between energy exerted and material removed. Energy per impact would be kept constant while investigating the impact frequency. When this relationship has been characterized, implications on ergonomics and efficiency will be better understood.

Ultimately, further research must be conducted to verify that the current models for indentation geometry, crushing, and chipping remain true at elevated frequencies of impact. If there is a deviation from these models, the frequency at which they are deemed unreliable must be determined.

5.3 Contributions to Knowledge

This research has successfully demonstrated that high frequency demolition of concrete is possible, and the implementation of a multi-head chisel is functional. This innovative design has been proven to be effective and has the potential to greatly contribute to the future development of concrete demolition hammers. Standard philosophy concerning demolition hammers is to increase the impact energy to increase the machines demolition rate. Mechanical limitations of single hammer mechanisms are no longer a boundary when multiple hammer mechanisms are able to impact a single tipped, multi head, chisel.

6 References

Abudayyeh, O. M. A., Sawhney, A., El-Bibany, & Buchanan, D. (1998). Concrete Bridge Demolition Methods and Equipment. *Journal of Bridge Engineering, 3*(3), 117-125.

Aoyama, H. (2001). *Design of Modern Highrise Reinforced Concrete Structures*. London: Imperial College Press.

Atici, U., & Ersoy, A. (2008). Evaluation of destruction specific energy of fly ash and slag admixed concrete interlocking paving blocks (CIPB). *Construction and Building Materials, 22*(7), 1507-1514. doi:10.1016/j.conbuildmat.2007.03.028

Benjumea, R., & Sikarskie, D. L. (1969). A note on the penetration of a rigid wedge into a nonisotropic brittle material. *International Journal of Rock Mechanics and Mining Sciences & Geomechanics Abstracts, 6*(4), 343-352. doi:http://dx.doi.org/10.1016/0148-9062(69)90038-2

Blitz, J., & Simpson, G. (1996). *Ultrasonic methods of non-destructive testing*. London; New York: Chapman & Hall.

Brooks, J. J. (2015). Elasticity of Concrete *Concrete and Masonry Movements* (Vol. 4, pp. 61-93). Oxford United Kingdon: Butterworth-Heinemann.

Carino, N. J., Guthrie, W. F., & Lagergren, E. S. (1994). *Effects of testing variables on the measured compressive strength of high-strength (90 MPa) concrete*. [Gaithersburg, MD]: U.S. Dept. of Commerce, National Institute of Standards and Technology Retrieved from http://books.google.com/books?id=ReZIAQAAIAAJ.

Carpenter, C. (2018). Complaints of noise pollution over Turcot Interchange construction prompts change. Retrieved from Global News website: https://globalnews.ca/news/4010103/complaints-of-noise-pollution-over-turcot-interchange-construction-prompts-change/

Caterpillar. (2019, January). Attachments, Hammers. Retrieved from https://www.cat.com/en_US/products/new/attachments/hammers.html

Che, D., Zhu, W.-L., & Ehmann, K. F. (2016). Chipping and crushing mechanisms in orthogonal rock cutting. *International Journal of Mechanical Sciences, 119*, 224-236. doi:http://dx.doi.org/10.1016/j.ijmecsci.2016.10.020

Chen, X., Ge, L., Zhou, J., & Wu, S. (2017). Dynamic Brazilian test of concrete using split Hopkinson pressure bar. *Mater Struct Materials and Structures, 50*(1), 1-15.

Cho, Y. S., Lee, S. I., & Bae, J. S. (2014). Reinforcement Placement in a Concrete Slab Object Using Structural Building Information Modeling. *Computer-Aided Civil and Infrastructure Engineering, 29*(1), 47-59. doi:10.1111/j.1467-8667.2012.00794.x

Copeman, W. S. C. (1940). The Arthritic Sequelae of Pneumatic Drilling. *Annals of the Rheumatic Diseases, 2*(2), 141-146. doi:10.1136/ard.2.2.141

Dawood, M., Ozerkan, N. G., Belarbi, A., Gencturk, B., Sohail, M. G., Kahraman, R., & Alnuaimi, N. A. (2018). Reinforced Concrete Degradation in the Harsh Climates of the Arabian Gulf: Field Study on 30-to-50-Year-Old Structures. *Journal of Performance of Constructed Facilities, 32*(5). Retrieved from doi:10.1061/(ASCE)CF.1943-5509.0001204

Dutta, P. K. (1972). A theory of percussive drill bit penetration. *International Journal of Rock Mechanics and Mining Sciences and Geomechanics Abstracts, 9*(4), 543-544. doi:10.1016/0148-9062(72)90044-7

El-Salakawy, E. F., Polak, M. A., & Soudki, K. A. (2002). Rehabilitation of reinforced concrete slab–column connections. *Canadian Journal of Civil Engineering, 29*(4), 602-611. Retrieved from doi:10.1139/l02-045

Fam, A. G., & Kolin, A. (1986). Unusual metacarpophalangeal osteoarthritis in a jackhammer operator. *Arthritis and rheumatism, 29*(10), 1284-1288.

Flowfit. (2017). Flowfit Technical Data Sheet Series 60000 PTO Gearbox Pump Retrieved from flowfitonline website: https://www.flowfitonline.com/search?open_pdf=1&name=/PGPA1.pdf

Gambatese, J. A. (2003). Controlled Concrete Demolition Using Expansive Cracking Agents. *Journal of Construction Engineering and Management, 129*(1), 98-104.

Gannoruwa, A. & Ruwanpura, J. (2007). Construction noise prediction and barrier optimization using special purpose simulation. *IEEE. Proc. 39th Conference Winter Simulation*. (pp. 2073-2081). IEEE. doi:10.1109/WSC.2007.4419839

Guo, Z. (2014). *Guo, Zhenhai. Principles of Reinforced Concrete. , 2014. Internet resource.*

Harada, T., Idemitsu, T., & Watanabe, A. (1985). Demolition of concrete with expansive demolition agent. *Doboku Gakkai Ronbunshu Doboku Gakkai Ronbunshu, 360*(360), 61-70.

Harada, T., Idemitsu, T., Watanabe, A., & Takayama, S.-i. (1989). The Design Method for the Demolition of Concrete with Expansive Demolition Agents. In S. P. Shah & S. E. Swartz (Eds.), *Fracture of Concrete and Rock: SEM-RILEM International Conference* (pp. 47-57). New York, NY: Springer New York.

Hilti. (2019, January). Demolition Hammers and Breakers. Retrieved from https://www.hilti.ca/c/CLS_POWER_TOOLS_7124/CLS_DEMOLITION_HAMMER_BREAKER_SUB_7124/CLS_DEMOLITION_HAMMER_BREAKER_7124#nav/close

Hua-Peng, C., Chen, H. & Nan, X. (2012). Analytical solutions for corrosion-induced cohesive concrete cracking. *Journal of Applied Mathematics, 2012*. doi:10.1155/2012/769132

King, C. I. (1894). United States Patent No. US513941A Retrieved from https://patents.google.com/patent/US513941

Larrard, F. & Colina, H. (2019). *Introduction in Concrete Recycling: Research and Practice* (pp. 3-5). Boca Raton, FL: CRC Press/Taylor & Francis Group. (2019).

Liao, K.-Y., Chang, P.-K., Peng, Y.-N., & Yang, C.-C. (2004). A study on characteristics of interfacial transition zone in concrete. *Cement and Concrete Research, 34*(6), 977-989. doi:10.1016/j.cemconres.2003.11.019

Mallinson, L. G., Davies, I. L., Commission of the European Communities. Directorate-General for Telecommunications, I. I., & Innovation. (1987). *A historical examination of concrete : final report*. Luxembourg: Commission of the European Communities

Mendis, P. (2003). Design of high-strength concrete members: state-of-the-art. *Progress in Structural Engineering and Materials, 5*(1), 1-15. doi:10.1002/pse.138

Miller, M. H., & Sikarskie, D. L. (1968). On the penetration of rock by three-dimensional indentors. *International Journal of Rock Mechanics and Mining Sciences and Geomechanics Abstracts, 5*(5), 375-398. doi:10.1016/0148-9062(68)90043-0

Momber, A. W. (2005). CHAPTER 1 - Introduction *Hydrodemolition of Concrete Surfaces and Reinforced Concrete* (pp. 1-22). Oxford: Elsevier Science.

Pang, S. S. (1987). *Investigations of pneumatic percussive processes involving rocks.* (Ph.D.), University of California, Berkeley, Ann Arbor. (8726329)

Pang, S. S., & Goldsmith, W. (1990). Investigation of crack formation during loading of brittle rock. *Rock Mech Rock Engng Rock Mechanics and Rock Engineering, 23*(1), 53-63.

Pang, S. S., & Goldsmith, W. (1992). A model of a pneumatic jackhammer system. *Rock Mechanics and Rock Engineering, 25*(1), 49-61. doi:10.1007/bf01041875

Pang, S. S., Goldsmith, W., & Hood, M. (1989). A force-indentation model for brittle rocks. *Rock Mechanics and Rock Engineering, 22*(2), 127-148. doi:10.1007/bf01583958

Pothisiri, T., & Panedpojaman, P. (2012). Modeling of bonding between steel rebar and concrete at elevated temperatures. *Construction and Building Materials, 27*(1), 130-140. doi:http://dx.doi.org/10.1016/j.conbuildmat.2011.08.014

Sataloff, J., Sataloff, R. T., Menduke, H., Yerg, R., & Gore, R. P. (1984). Hearing loss and intermittent noise exposure. *Journal of occupational medicine. : official publication of the Industrial Medical Association, 26*(9), 649-656.

Shields, P. G., & Chase, K. H. (1988). Primary torsion of the omentum in a jackhammer operator: another vibration-related injury. *Journal of occupational medicine. : official publication of the Industrial Medical Association, 30*(11), 892-894.

Suprenant, B. (1991, August). Choosing a demolition hammer. *Concrete Repair Digest,* 2(4), 101.-103.

Tool, N. (2015). Ironton Demolition Breaker Owner's Manual. Retrieved from https://www.northerntool.com/images/downloads/manuals/46479.pdf

Wache, R. (2000). European Patent No.EP105207B1. Retrieved from https://patents.google.com/patent/EP1052070B1/en?q=sds&q=plus&oq=sds+plus

Wang, X. & Su, O. (2019). Specific energy analysis of rock cutting based on fracture mechanics: A case study using a conical pick on sandstone. *Engineering Fracture Mechanics, 213*, 197-205. doi:10.1016/j.engfracmech.2019.04.010

7 Appendices

7.1 Appendix A. Moil Point and Cold Chisel Design

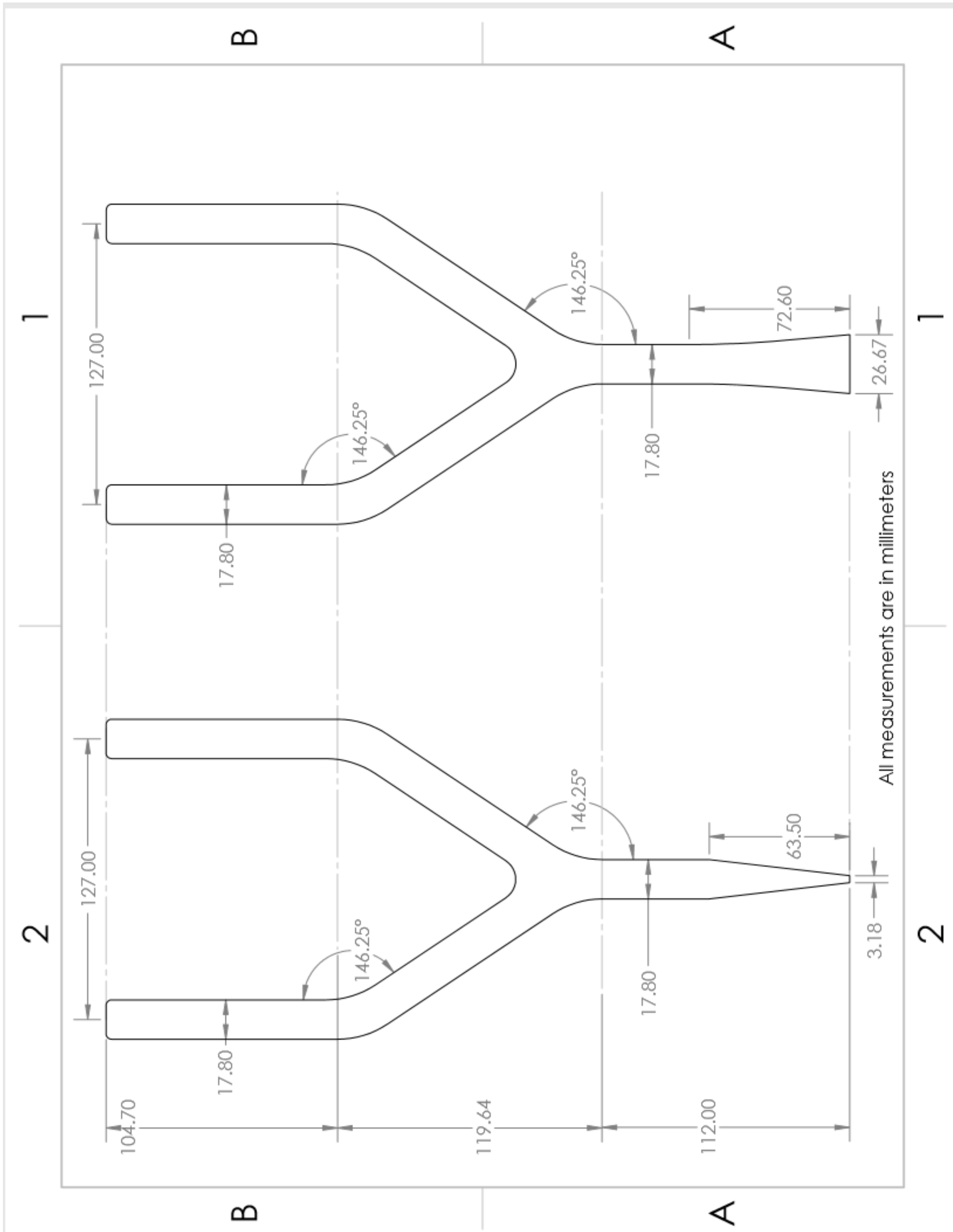

Figure 7.1.1 Chisel design Cold Chisel-1 Moil Point Chisel-2

7.2 Appendix B. Ironton Parts and Assembly Diagram

DIAGRAM AND PARTS LIST

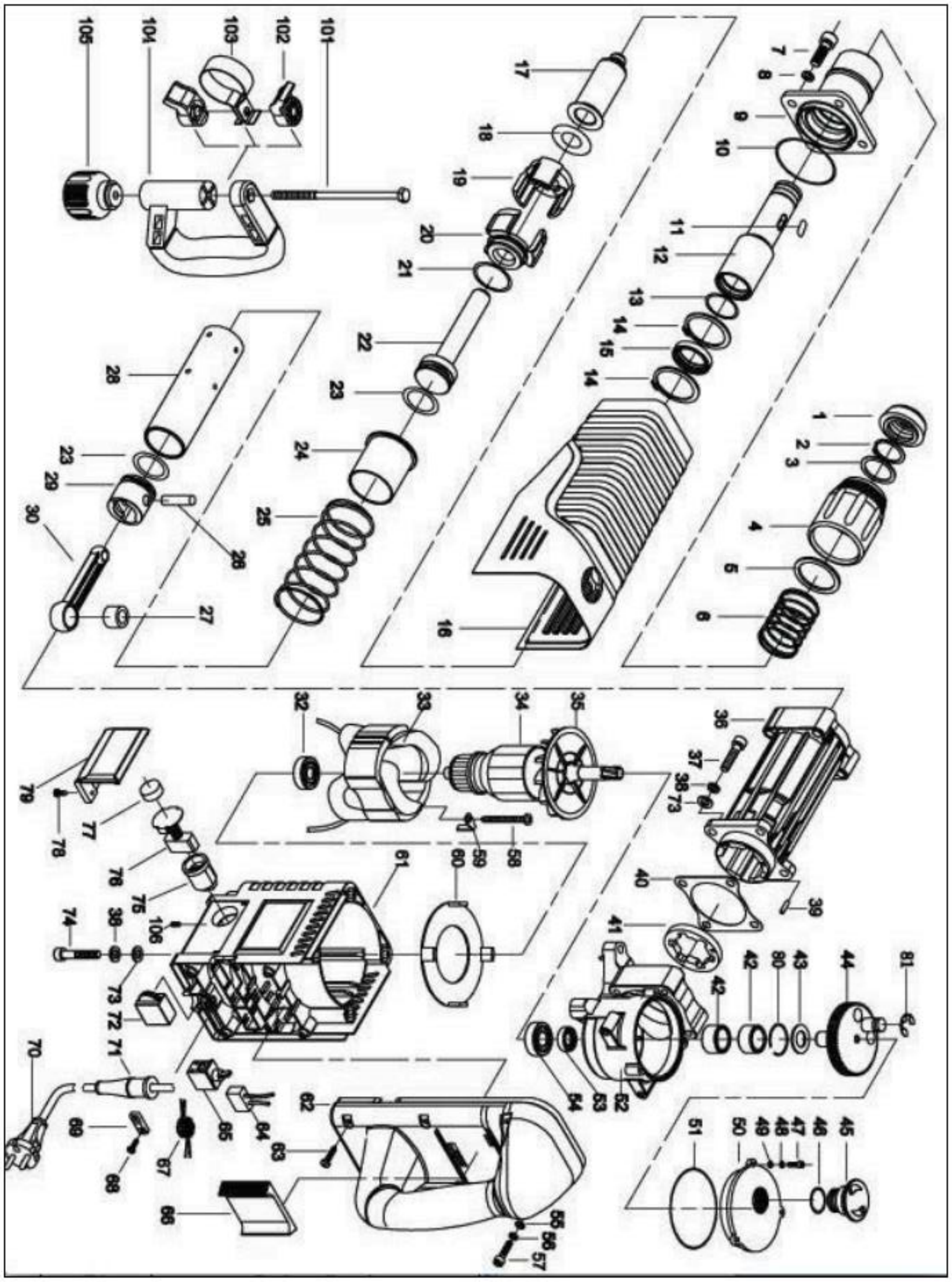

Figure 7.2.1 Ironton Parts Diagram (Tool, 2015)

NO.	PART DESCRIPTION	NO.	PART DESCRIPTION
1	Front Cover	45	Oil Cap
2	Axile Circlip φ28	46	O-Ringφ27×φ2
3	Circlip φ38.5×φ37.5×1.5	47	Bolt M4×14
4	Slider	48	Spring Washerφ4
5	Spring Washer	49	Washerφ4
6	Spring	50	Top Cover
7	Bolt M10×30	51	O-Ringφ84×φ1.5
8	Spring Washerφ10	52	Wheel Box
9	Tool Holder	53	Oil Seal
10	O-Ring φ69×φ2	54	Bearing 6202
11	Steel Ball Poleφ8×19.5	55	Washerφ6
12	Guard Ring Sleeve	56	Spring Washer φ6
13	O-Ring φ37×φ2.5	57	Bolt M6×25
14	Circlipφ41	58	Tap Bolt ST4.8×65
15	Oil Seal Ferrule	59	Stator Holding Plate
16	Shell	60	Air Baffle
17	Second Striker	61	Motor Housing
18	Anti-Vibration Ring	62	Rear Handle
19	Guide Sheath	63	Tap Bolt ST4.8×25
20	Cylinder Connector	64	Capacitance
21	O-Ring φ43×φ3	65	Switch
22	Ram	66	Slide Switch
23	O-Ringφ40×φ5	67	Inductance
24	Control Bush	68	Tap Bolt ST4.2×16
25	Compress Spring	69	Cable Clamp
26	Piston Pin	70	Cable（3M）
27	Needle Bearing NK14/16	71	Cable Sheath
28	Cylinder	72	Speed Control
29	Piston	73	Washer φ8
30	Connecting Rod	74	Bolt M8×45
32	Bearing 6201	75	Brush Holder
33	Stator	76	Carbon Brush
34	Rotor	77	Brush Cap
35	Fan	78	Tap Bolt ST4.2×13
36	Cylinder Case	79	Decoration Cover
37	Bolt M8×45	80	Circlipφ29Xφ1.5
38	Spring Washerφ8	81	Circlipφ12
39	Pin B4X16	101	Bolt M8×140
40	Seal Washer	102	Clamp
41	Holding Plate	103	Chuck Ring
42	Centripetal Needle Holder A'sy K16×22×15	104	Auxiliary Handle
43	Adjustment Washer	105	Knob
44	Big Gear	106	Screw M5X10

Figure 7.2.2 Ironton 46479 Parts List (Tool, 2015)

7.3 Appendix C. Flowfit 1:3.8 Gear Box

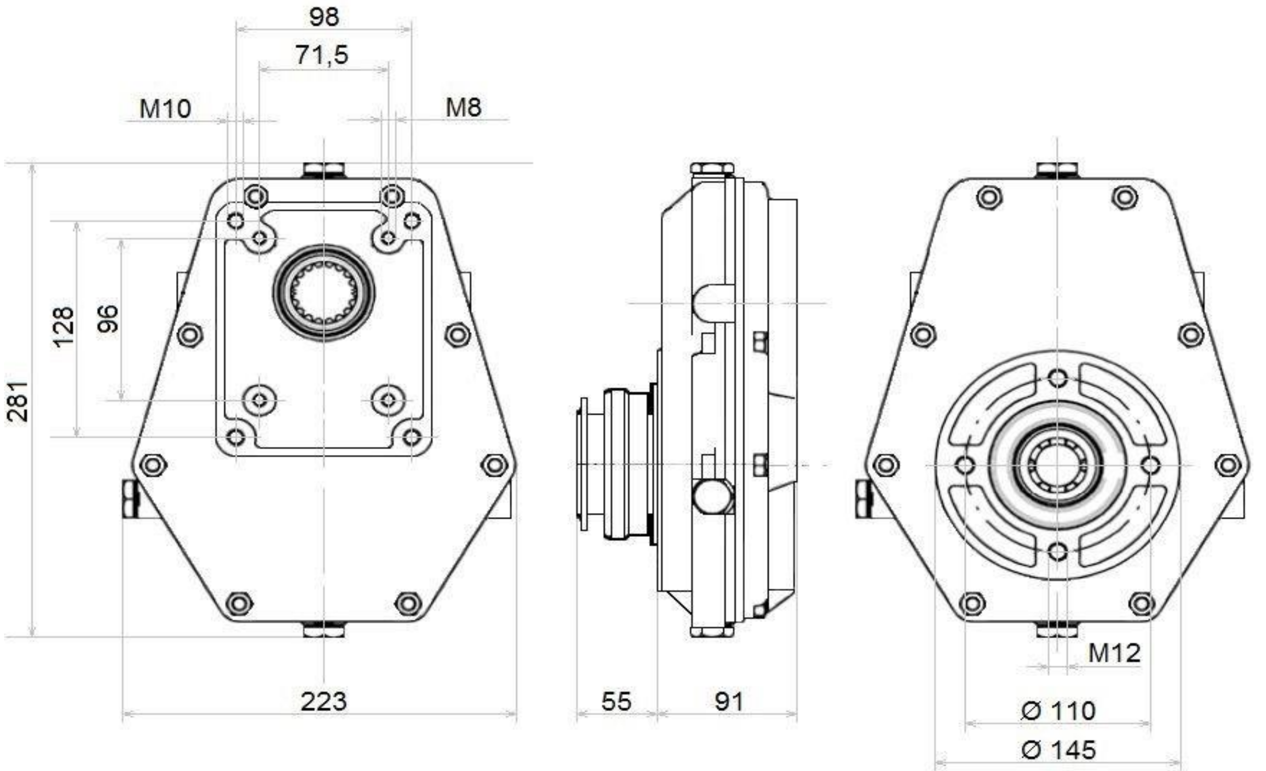

Figure 7.3.1 Flowfit Gearbox(Flowfit, 2017) (all measurements in mm)

7.4 Appendix D. Hydraulic Flow Diagram

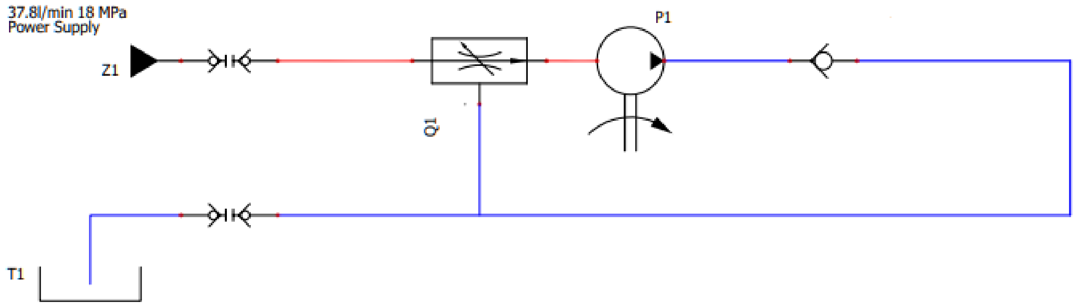

Figure 7.4.1 Hydraulic Flow Diagram for Hydro-Mechanical Jackhammer

- Q1- Compensated Flow Control Valve
- P1- Haldex Gear Pump. Maximum Rotational Speed of 3600 RPM
- Z1- Hydraulic Power Connection
- T1- Low Pressure Return to Sump